RANGELAND RESOURCE ASSESSMENT ACROSS THE AFRICA CONTINENT FOR IMPROVED ECOSYSTEM HEALTH AND SUSTAINABLE FOOD SYSTEMS

GMV and ILRI, 2022

gmv INNOVATING SOLUTIONS
ILRI INTERNATIONAL LIVESTOCK RESEARCH
CGIAR INITIATIVE ON Livestock and Climate
CGIAR INITIATIVE ON Climate Resilience

TABLE OF CONTENTS

LIST OF FIGURES AND TABLES

1. INTRODUCTION

1.1. PURPOSE

This assessment was commissioned by UNEP Kenya and contributes to the UN resolution 2/24 on combating desertification, land degradation and drought and promoting sustainable pastoralism and rangelands; and UN resolution 4/15 on innovations in sustainable rangelands and pastoralism, as well as the UNEP-led gap analysis on rangelands and the resulting report: *Rangelands: A case of benign neglect* and is a valuable input to the UN Decade for Ecosystem Restoration.

This rangeland resource assessment also compliments the global Rangelands Atlas produced in 2021 as a collaboration between UNEP, ILRI and other stakeholders; contribute to a baseline for the development of a GEF-funded global project on rangeland restoration and the development of a rangeland monitoring system for Africa led by the European Space Agency and a global rangelands data platform led by ILRI. This research also contributes to the Livestock and Climate initiative and the Climate Security initiative of the One CGIAR. GMV and ILRI thank all funders who supported this research.

More broadly the assessment contributes to discussions and interventions focusing on One Health, with rangelands health being an important pillar of this, as well as sustainable food systems. This includes attention to such as land degradation, climate impacts on livestock and other environmental challenges, and allow better analyzing opportunities for more sustainable investments in rangelands through restoration or other and livestock production systems.

1.2. SCOPE AND OBJECTIVES

The scope of the assessment is on the African continent and includes the following activities:

- Link between rangelands degradation and environmental threats/climate hazards

This is accomplished by an historic analysis of the rangeland dynamics over Africa. In particular, the project analysed the existing land cover types and land cover transitions experienced in the last 30 years (1992-2020) over the African rangelands.

- Nexus between rangelands, One Health, and sustainable food systems

Two studies are developed on this topic.

1. Analysis of the climate change impact on the heat stress in livestock species over Africa. The heat stress is estimated using meteorological reanalysis for the historic period, and the projected heat stress is computed using regional climate models for Africa. The risk factor per country is calculated aggregating the information per country considering weights for the livestock distribution over the rangelands.
2. Estimation of the Human Appropriation of Net Primary Productivity (HANPP) for rangelands. The HANPP provides a useful measure of human intervention into the African rangelands. This index is computed using FAOSTAT information, dynamic global vegetation models (DGVM), and satellite data.

All these datasets, but the HANPP, are included into an interactive web-based app developed in the context of this activity allowing exploring the results over any African country for any year of the period considered. In addition, the results for two specific countries, Senegal and Ethiopia, are discussed in this document to showcase the analysis that can be done using the online application.

1.3. ACRONYMS

Table 1-1 Acronyms

Acronym	Definition
APAR	Absorbed Photosynthetically Active Radiation
AVHRR	Advanced Very-High-Resolution Radiometer
C3S	Copernicus Climate Change
CCI	Climate Change Initiative
CGLS	Copernicus Global Land Service
CMIP5	Coupled Model Intercomparison Project Phase 5
CORDEX	Coordinated Regional Climate Downscaling Experiment
DGVM	Dynamic Global Vegetation Models
ECMWF	European Centre for Medium-Range Weather Forecasts
ESA	European Space Agency
FAO	Food and Agriculture Organization of the United Nations.
GCM	Global Climate Model
GCP	Google Cloud Platform
GDP	Gross Domestic Product
GEE	Google Earth Engine
GEF	Global Environmental Facility
GIS	Geospatial Information System
GLW	Gridded Livestock of the World
GNI	Gross National Income
HANPP	Human Appropriation of Net Primary Productivity
ILRI	International Livestock Research Institute
IPCC	International Panel on Climate Change
ISIMIP	Inter-Sectoral Impact Model Intercomparison Project
LAI	Leaf Area Index
LC	Land Cover
LCSS	Land Cover Classification System
MERIS	Medium Resolution Imaging Spectrometer
MODIS	Moderate Resolution Imaging Spectroradiometer
NPP	Net Primary Productivity
PSN	Photosynthesis
RCM	Regional Climate Model
RCP	Representative Concentration Pathway
THI	Temperature Humidity Index
UN	United Nations

UNEP	United Nations Environmental Programme
WWF	World Wildlife Fund

2. WEB-BASED APPLICATION TO EXPLORE RANGELANDS DATA OVER AFRICA

The objective of this project is to assess the resources available to analyze the current situation, the expected future condition, and the dynamics experienced over the last decades, for the different rangeland types in Africa. These include existing datasets and the elaboration of new products taking advantage of the work developed by international institutions and programs that monitor and forecast the state of the ecosystems, to support climate change mitigation and adaptation strategies.

The geographical coverage of this assignment is vast, more than 29.2 million km² of rangeland systems, and it covers all the countries within the African continent: 54 countries in Africa today, according to the United Nations. The analysis of results at that scale through maps or graphs is of limited value due to the loss of details when the aggregation of results is performed to allow the visualization and interpretation. Instead of presenting a catalogue of maps and statistics as the main outcome of this project, the GMV team, in agreement with ILRI, decided to prepare a simple web-app to go beyond the initial idea and allow users to explore their data of interest on rangelands themselves.

This new app fully compliments the global Rangelands Data Platform in development. The focus of the Atlas is on presenting global information for rangelands linked to use stories that demonstrate the importance of rangelands and highlight the changes taking place which are having significant impacts on rangelands, demanding their protection and restoration. The web-app developed under this assignment presents, instead, a basic geospatial platform with common GIS functionalities that permits the detailed exploration of the long timeseries of rangeland datasets implemented in the catalogue over Africa. The platform's aim is to allows users researching on rangelands and comparing situations for different periods/ datasets/ countries in a friendly and fast way. In a second phase, the data available under the Rangelands Atlas could be also added to the resources of this new web-app.

Taking advantage of the existing collaboration framework between GMV and Google (GMV belongs to the Earth Engine Partner Initiative), the GMV team developed a GIS platform as a web-based app in the environment of Google Earth Engine (GEE). This app grants free access (no need of user login) and easy visualization of the datasets implemented. Some of these datasets are available in the GEE catalogue (no cost), but most of them are datasets developed "ad-hoc" for this assignment, stored in Google Cloud Platform (GCP) and accessed via GEE. The maintenance cost of the current datasets related to the GCP storage is, however, negligible.

The platform can be accessed through this temporary link. We aim that the platform, or the functionalities and products existing in the platform, will be hosted by the Global Rangelands Data platform which for now will be administered by ILRI.

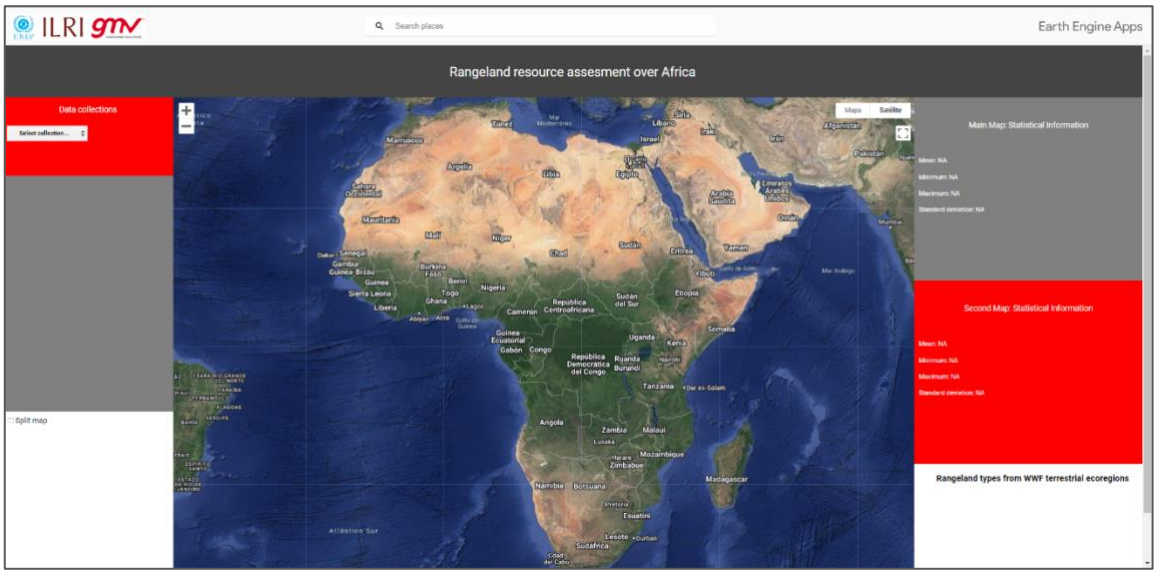

Figure 2-1 Snapshot of the web-app

The following sections describe the different datasets included in the web-app and the current features and functionalities for each dataset. The data source and description are given for the datasets coming from existing resources, and the methodology and results are described for the ad-hoc datasets incorporated into the platform.

Note that the web-app tool counts with the generic Google GIS tools such as zoom in/out, possibility to select the background map, that is satellite (with the option to enable or disable tags) or default map (with the option to enable or disable terrain lines), full screen mode, or a search bar to find spots by name.

The box "Layers" shows the loading bars of the different geospatial layers requested by the user after a query. Once the loading bars are complete all the layers of the user's query are uploaded and displayed.

2.1. RANGELAND TYPES

According to the Rangelands Atlas (https://hdl.handle.net/10568/114064), rangelands can be described as land on which the vegetation is predominantly grasses, grass-like plants, forbs, or shrubs, and often with trees that are grazed or have the potential to be grazed by livestock and wildlife. This is the definition employed in this assessment, and the selection of rangeland types for Africa follows the approach taken in the Atlas. Five of fourteen biomes or rangeland types made up of terrestrial ecoregions as defined by WWF has been selected.

Figure 2-3 presents the five rangeland types used in this assignment:

- Tropical and subtropical grasslands, savannas and shrublands
- Flooded grasslands and savannas
- Montane grasslands and shrublands
- Mediterranean forest, woodlands, and scrubs
- Deserts and xeric shrublands

The rangeland types are not shown as a product in the catalogue of the web-app. That is, they cannot be selected in the data collection dialogue. Instead, the rangeland types are used as the

baseline maps that mask out all the other products allowing focusing the analysis over rangelands.

The rangeland types present per country are shown in the right bottom panel “Rangeland types from WWF Terrestrial ecoregions” after selecting the African country of interest. Users can show or hide the different layers as preferred.

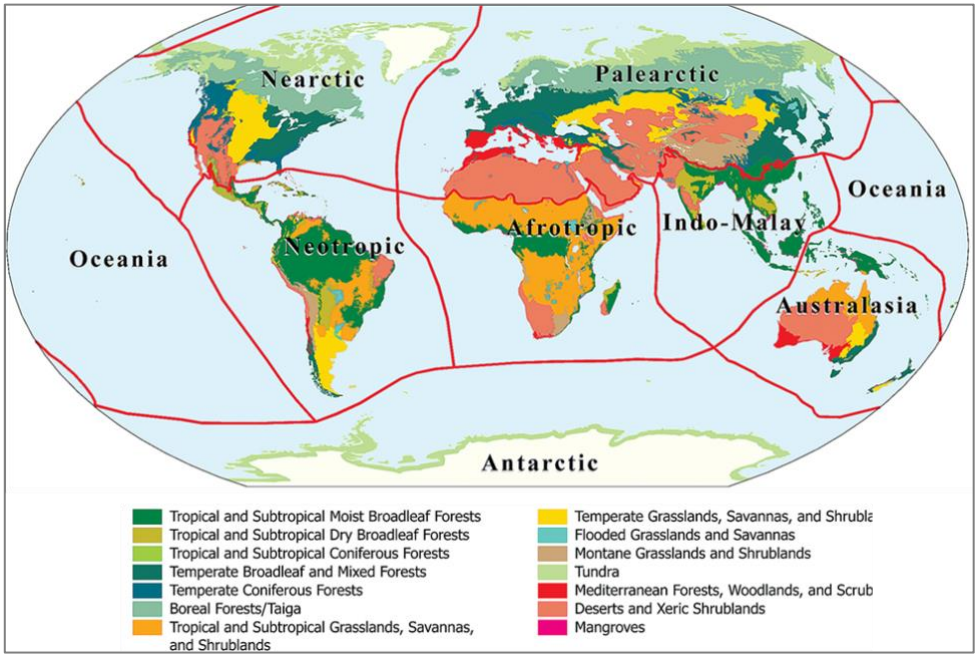

Figure 2-2 WWF terrestrial ecoregions. For more information see:
https://www.worldwildlife.org/publications/terrestrial-ecoregions-of-the-world

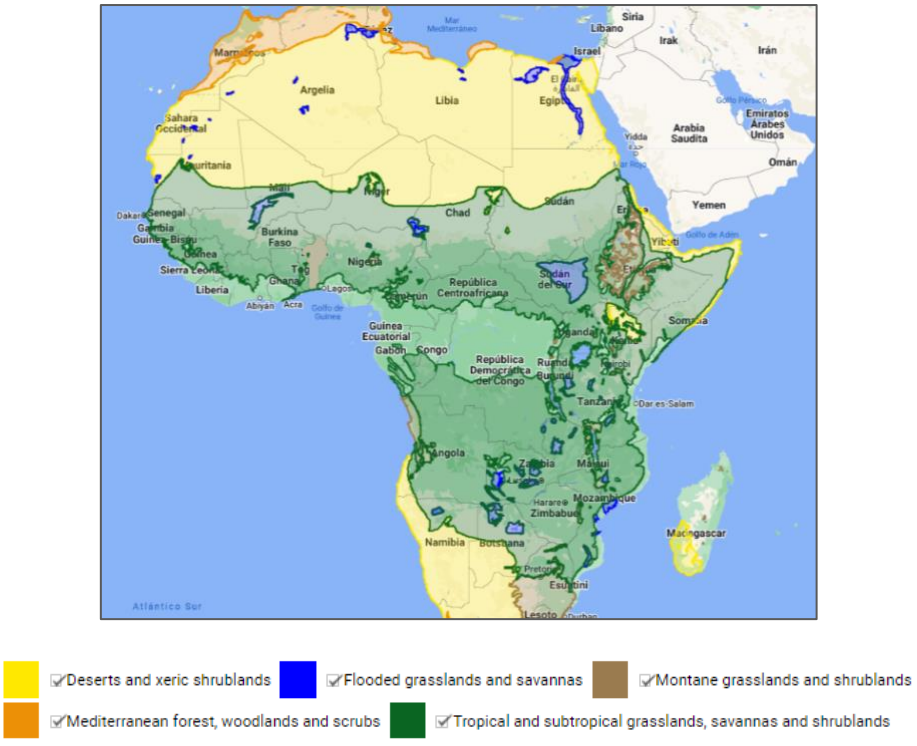

Figure 2-3 Rangeland types selected for this assignment.

2.2. LAND COVER

The web-app incorporates the information for Africa of the Land cover (LC) classification gridded maps from the Copernicus Climate Change (C3S) service. The C3S provides global LC maps from 1992 to 2020 at 300m spatial resolution that describe the land surface following the UN Land Cover Classification System (LCCS). These land cover maps are entirely consistent with the timeseries of the global annual LC maps produced by the ESA Climate Change Initiative (CCI). To produce this dataset, the entire Medium Resolution Imaging Spectrometer (MERIS) archive from 2003 to 2012 was first classified into a unique 10-year baseline LC map. This is then back- and up-dated using change detected from:

- Advanced Very-High-Resolution Radiometer (AVHRR) time series from 1992 to 1999
- SPOT-Vegetation (SPOT-VGT) time series from 1998 to 2012
- PROBA-Vegetation (PROBA-V) and Sentinel-3 OLCI (S3 OLCI) time series from 2013.

This dataset provides long-term consistency, yearly updates, and high thematic detail on a global scale is, therefore, well-suited for monitoring rangeland systems. Being the analysis of the long-term changes in rangelands of great interest for users according to the user interview results from previous projects, it was decided to include it as a reference in the platform.

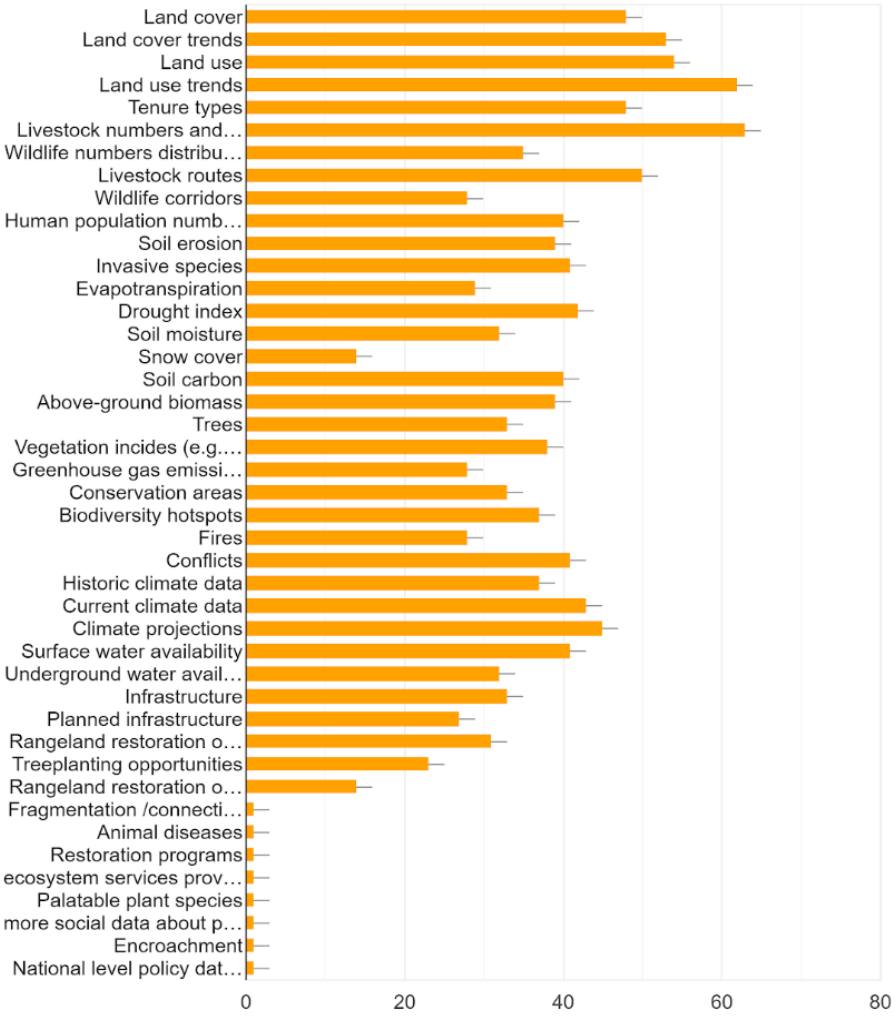

Figure 2-4 Results to the question "if the Rangelands Data Platform provided information on the following would you use this data? [Check the ones that you would use]" in the context of the questionnaire launched to the rangeland community in the project Building Resilience in Rangeland Communities with Big data led by ILRI.

2.2.1. AVAILABLE FEATURES

The land cover maps are presented in the platform as shown in the example depicted in Figure 2-5.

Users can select any year from 1992 to 2020, and the country of interest. After pressing "Apply layer", the existing land cover classes for that year and country are mapped. Note that the information is only shown over the rangeland systems present in Africa as described in section 2.1. The coverage (in km2) of each land cover class over rangelands is computed and shown in the right top panels.

Rangeland systems present in the country are shown in the right bottom panel. To visualize them users should press "Show" button, this will overlay a semitransparent mask over the land cover map. Selecting and deselecting the rangeland layers will show or hide them. The coverage statistics can be customized per rangeland type, to do so the user must select the rangeland systems of interest and press "Apply layer" in the left panel. The web-app will automatically recalculate the areas for land cover classes only over the selected rangeland types.

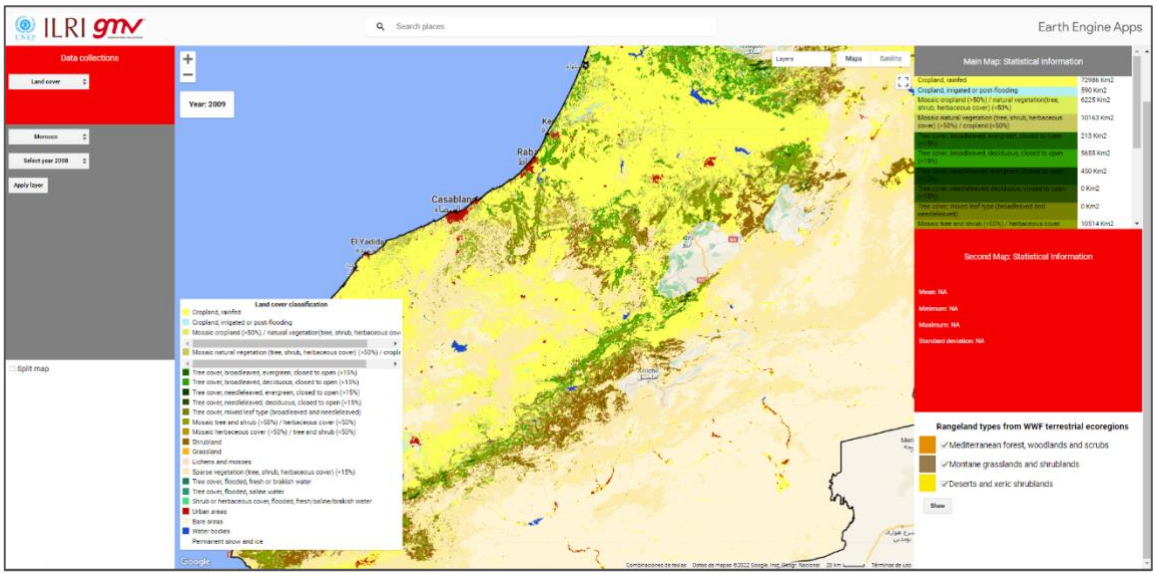

Figure 2-5 Snapshot of the land cover product within the web-app.

The app allows to intercompare results for different years. To access to this functionality the user must select the "Split map" option, below the left panel. Then, select the country and the first year in the top left panel, and "Apply layer" to show the first map, and the second year of study in the bottom left panel, and "Apply layer" to show second map.

Figure 2-6 shows an example of Land cover maps over Kenya for 1998 and 2018 presented simultaneously. The horizontal scroll line allows scrolling left and right to quickly analyze changes in the two years selected. The area statistics of the two maps are shown in the right statistical panels. In the split mode, user can also select certain rangeland layers are recalculate the coverage statistics by pressing the corresponding "Apply layer" buttons in the left panels.

Figure 2-6 Snapshot of the land cover product in the split mode.

2.3. LAND COVER TRANSITIONS

The web-based app includes not only the land cover classification maps of the last 30 years, but also all the transitions experienced over the rangeland ecosystems in Africa.

The definition of the land cover transitions is derived from the Copernicus Global Land Service (CGLS). The matrix of the land cover transitions is shown in Table 2-1.

Table 2-1 Matrix of LC transformation processes.

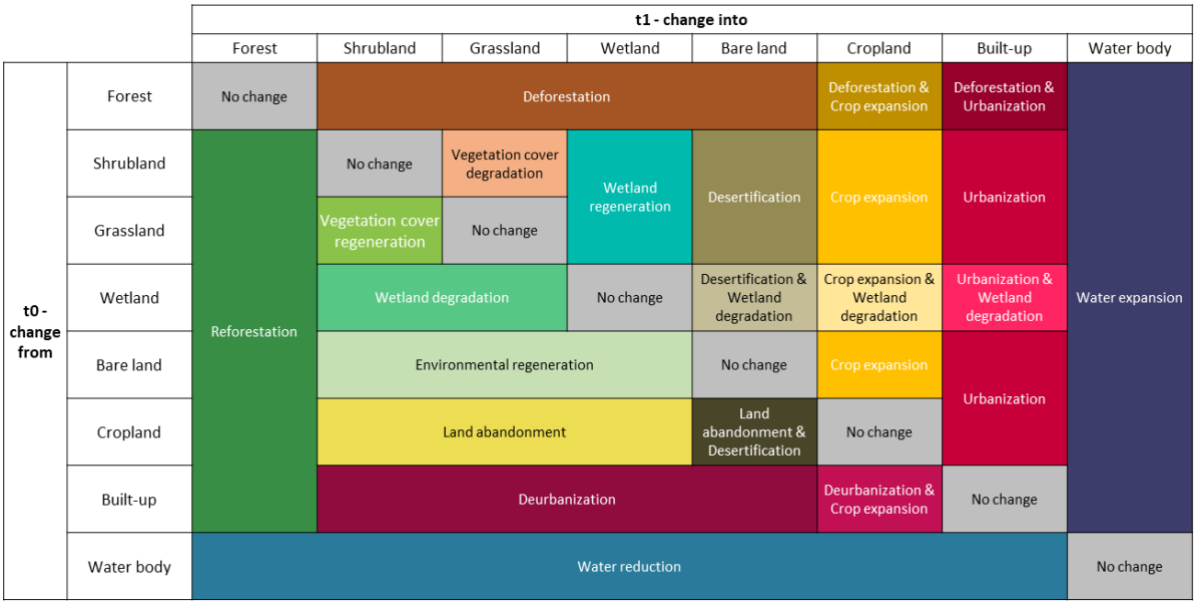

To facilitate the analysis of the transformation processes the land cover classes from the original ESA CCI definition have been assigned to the IPCC classes considered for the change detection. Note that the correspondence of land cover classes is provided by the ESA CCI Land Cover team.

The new land cover classes align well with the ones used by the Copernicus Land Cover transitions. However, sparse vegetation is not considered. Therefore, following Radwan et al. 2021, the sparse vegetation class is included in bare soil. The new classification is given in Table 2-2.

Table 2-2 Land cover reclassification.

Colour	Original C3S Land Cover classes	IPCC reclassified classes
	Cropland, rainfed	Cropland
	Herbaceous cover	Cropland
	Tree or shrub cover	Cropland
	Cropland, irrigated or post-flooding	Cropland
	Mosaic cropland (>50%) / natural vegetation (tree, shrub, herbaceous cover) (<50%)	Cropland
	Mosaic natural vegetation (tree, shrub, herbaceous cover) (>50%) / cropland (<50%)	Cropland
	Tree cover, broadleaved, evergreen, closed to open (>15%)	Forest
	Tree cover, broadleaved, deciduous, closed to open (>15%)	Forest
	Tree cover, broadleaved, deciduous, closed (>40%)	Forest
	Tree cover, broadleaved, deciduous, open (15-40%)	Forest
	Tree cover, needleleaved, evergreen, closed to open (>15%)	Forest
	Tree cover, needleleaved, evergreen, closed (>40%)	Forest

	Tree cover, needleleaved, evergreen, open (15-40%)	Forest
	Tree cover, needleleaved, deciduous, closed to open (>15%)	Forest
	Tree cover, needleleaved, deciduous, closed (>40%)	Forest
	Tree cover, needleleaved, deciduous, open (15-40%)	Forest
	Tree cover, mixed leaf type (broadleaved and needleleaved)	Forest
	Mosaic tree and shrub (>50%) / herbaceous cover (<50%)	Forest
	Tree cover, flooded, fresh or brakish water	Forest
	Tree cover, flooded, saline water	Forest
	Mosaic herbaceous cover (>50%) / tree and shrub (<50%)	Grassland
	Grassland	Grassland
	Shrub or herbaceous cover, flooded, fresh/saline/brakish water	Wetland
	Urban areas	Built-up
	Shrubland	Shrubland
	Evergreen shrubland	Shrubland
	Deciduous shrubland	Shrubland
	Lichens and mosses	Bare land
	Sparse vegetation (tree, shrub, herbaceous cover) (<15%)	Bare land
	Sparse tree (<15%)	Bare land
	Sparse shrub (<15%)	Bare land
	Sparse herbaceous cover (<15%)	Bare land
	Bare areas	Bare land
	Consolidated bare areas	Bare land
	Unconsolidated bare areas	Bare land
	Water bodies	Water body

2.3.1. AVAILABLE FEATURES

The land cover transition maps are presented in the platform as shown in the example displayed in Figure 2-7.

Users should select two years between 1992 and 2020, and the country of interest. After pressing “Apply layer”, the land cover transitions between the two years selected for that country will be mapped. Note that the information is only shown over the rangeland systems present in Africa as described in section 2.1. The extent (in km2) of each transition class that occurred over the rangeland systems is computed and shown in the right top panel.

Rangeland systems present in the country are shown in the right bottom panel. To visualize them users should press the “Show” button, this will overlay a semitransparent mask over the land cover transition map. Selecting and deselecting the rangeland layers will show or hide them. The coverage statistics can be customized per rangeland type, to do so the user must select the rangeland systems of interest and press “Apply layer” in the left panel. The web-app will automatically recalculate the areas for land cover transition classes only over the selected rangeland types.

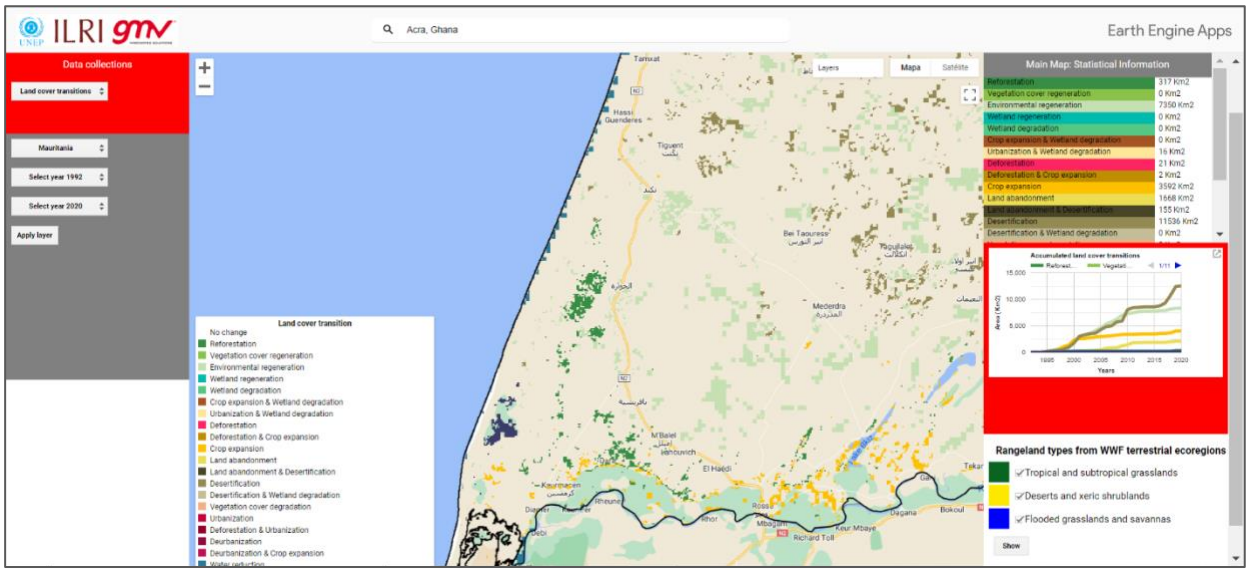

Figure 2-7 Snapshot of the land cover transition product within the web-app.

Once the period of interest is selected and the geospatial information displayed in the viewer, the yearly accumulated change extent for each land cover transition is presented in a graph in the middle right panel. The period analyzed corresponds to the period selected in the map. The horizontal arrows on the top of the graph allows the users to check all the existing transitions, while the top right arrow allows the user to display the graph in another tap of the browser to better visualize the results.

As already explained, the results provided by the tool are masked by the rangeland types as defined by WWF. This is also applicable to the results provided in the plots. The graph shows the accumulated changes that occurred over the rangeland types existing in the country. Users interested in analyzing results over certain rangeland types can disable the rangeland types out of their interest and press “Apply layer” to recalculate the results over their preferred areas.

As shown in Figure 2-8, the trend information can be downloaded as an image (either raster PNG file or vector SVG file), or in tabulated form as CSV.

It should be noted that the graph shows the accumulated changes between two timestamps for each of the transitions, while the table shows the transitions comparing only the two timestamps.

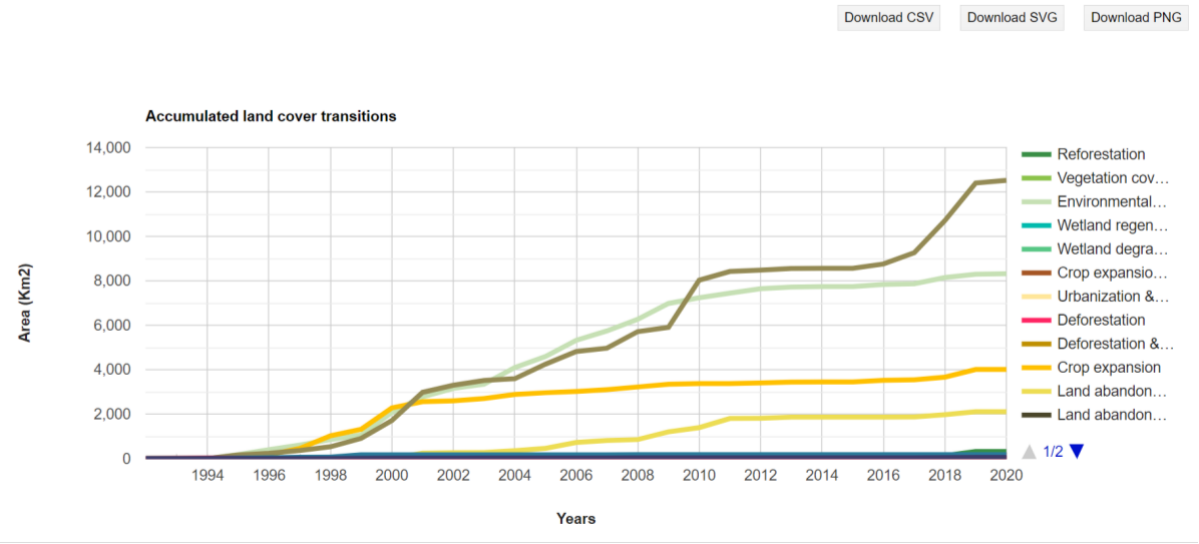

Figure 2-8 Snapshot of the trend analysis of the land cover transitions within the web-app.

2.4. HEAT STRESS IN LIVESTOCK

In the context of this activity, the team carried out an analysis of the climate change impact on the heat stress in livestock species (cattle, sheep, and goats) over Africa. These new datasets have been created ad-hoc for this study, covering both historical and future periods, and all the countries in Africa.

Heat stress in livestock is usually evaluated by use of different environmental variables (e.g., temperature, relative humidity, solar radiation, air movement or precipitation), either individually or combined into an index. The temperature humidity index (THI) combines the effect of air temperature and relative humidity and is considered to be a suitable indicator for assessing the level of heat stress on animals caused by weather conditions.

There are several THI equations for estimating the degree of thermal heat stress experienced by cattle, sheep, and goats. In this study we used the THI equations from Raimi et al., 2021.

For cattle, the THI was calculated using an equation developed for the Holstein-Friesian breed:

$$\boldsymbol{THI = (1.8 * Tmax + 32) - [(0.55 - 0.0055 * RH) * (1.8 * Tmax - 26.8)}$$

Where T_{max} is the daily maximum air temperature (ºC), and RH the relative humidity.

For sheep and goats, the THI was calculated using the livestock and poultry heat stress indices (LPHSI) from Marai et al., 2000:

$$\boldsymbol{THI = Tmax\ [(0.31 - 0.0031 * RH) * (Tmax - 14.4)]}$$

The degree of heat stress with corresponding THI value for different livestock is taken from Raimi et al., 2021 too (see Table 2-3). For cattle, we used thresholds proposed by Wiersma (1990), which have been used in many studies in tropical regions. For sheep and goat, we have modified thresholds proposed by Marai et al. (2000) which was used for male lambs, based on available studies about their upper critical temperature and their physiological responses under heat stress events.

Table 2-3 Degree of heat stress with corresponding THI value for cattle, sheep, and goats

	Cattle	Sheep	Goat
No stress	THI≤72	THI≤25	THI≤27
Mild	72<THI≤78	25<THI≤30	27<THI≤32
Moderate	78<THI≤88	30<THI≤35	32<THI≤37
Severe	THI>88	THI>35	THI>37

In Table 2-3, "no stress" means without heat stress and allowing livestock to be at optimum productive and reproductive performance, "mild" means with heat stress, but the livestock's body is able to control the heat stress by chemical and physical means, "moderate" means that the body temperature increases and can negatively impact the livestock's performance, and "severe' means events that result in significant decreases in productive and reproductive performances.

2.4.1. HISTORIC HEAT STRESS

The calculation of the historic record of heat stress in livestock is performed using the variables and the full period of ERA5-Land data, i.e., from 1950 to 2021. ERA5-Land is a meteorological reanalysis dataset that provides a consistent view of the evolution of land variables over several decades at 9km. ERA5-Land has been produced by replaying the land component of the ECMWF ERA5 climate reanalysis. This reanalysis combines model data with observations from across the world into a globally complete and consistent dataset using the laws of physics. ERA5-Land produces data that goes several decades back in time, providing an accurate description of the climate from the past to the present.

The THI values and indicators are available in the platform from 1950 until 2021. The values and indicators are computed daily at pixel level for every country in Africa, but the statistics are given at annual basis. Note that it is expected to additionally include seasonal statistics in following updates of the web-based app.

As an example, Figure 2-9 shows the degree of heat stress for cattle in Ethiopia in 1998. This information can be evaluated against the heat stress for any other year or compare with the situation for other livestock species in the same country.

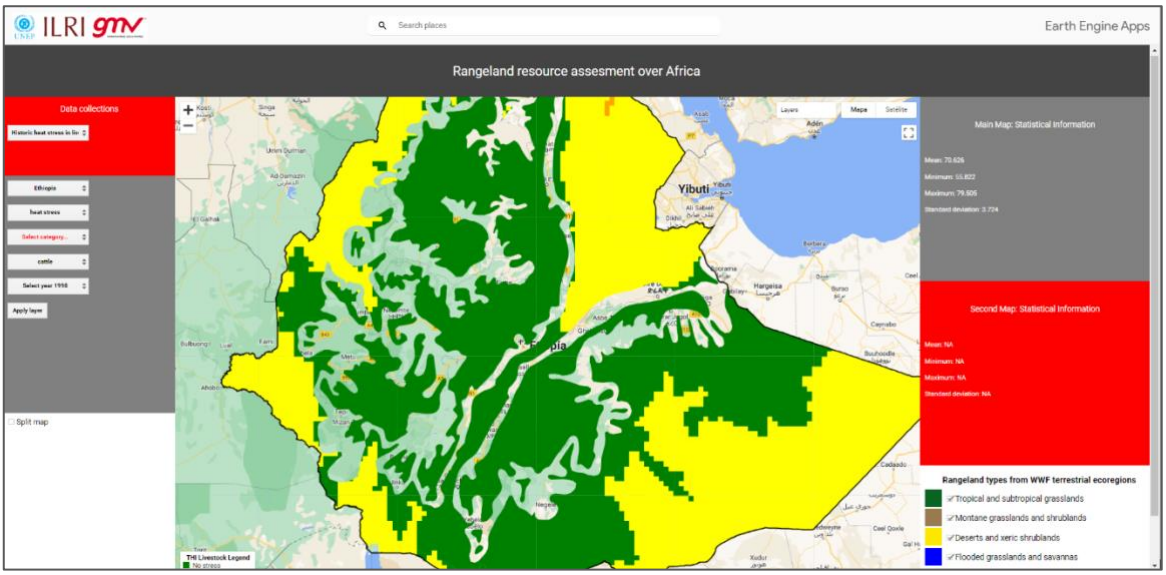

Figure 2-9 Snapshot of the historic heat stress in livestock product within the web-app.

ANTICIPATED HEAT STRESS

The calculation of the expected heat stress in livestock for Africa is performed using climate projections from the high-resolution Regional Climate Models (RCMs) of CORDEX Africa for the period 2030 – 2098.

RCMs provide climate change information on regional and local scales in relatively fine detail (0.22 degrees), which cannot be obtained from coarse scale Global Climate Models (GCMs). This is manifested in better description of small-scale regional climate characteristics and in more accurate representation of extreme events. RCMs are not independent from the GCMs, since the GCMs provide lateral and lower boundary conditions to the regional models.

The Coordinated Regional Climate Downscaling Experiment (CORDEX) consists of RCM simulations representing different future socio-economic scenarios (representative concentration pathways -RCPs-), different combinations of GCMs from the CMIP5 results, and RCMs and different ensemble members of the same GCM-RCM combinations.

In this activity, we have taken the RCPs 2.6 and 8.5, and the combination of GCM-RCM displayed in Table 2-4 to prepare the model ensemble for temperature and humidity and compute the heat stress index.

Table 2-4 Combination of GCM-RCM used in the calculation of the expected THI for livestock.

GCM	RCM
MOHC-HadGEM2-ES	CLMcom-KIT-CCLM5-0-15
	GERICS-REMO2015
	ICTP-RegCM4-7
NCC-NorESM1-M	CLMcom-KIT-CCLM5-0-15
	GERICS-REMO2015
	ICTP-RegCM4-7
MPI-M-MPI-ESM-LR	CLMcom-KIT-CCLM5-0-15
	GERICS-REMO2015
MPI-M-MPI-ESM-MR	ICTP-RegCM4-7

The daily values of the CORDEX ensemble selected, for the two RCPs, are averaged for the reference period (historic: 1950-2005) and for the following future periods: 2006-2029, 2030-2049, 2050-2069, and 2070-2098.

The heat stress and indicators are then computed for the five available periods and the two RCPs. The results can be shown for two “scenarios”, i) for each future period (climate projection), and ii) as the difference between the values and indicators in the projected periods and the same values in the reference period (difference with baseline), per country. The statistics are given at annual basis, but it is expected to additionally include seasonal statistics in following updates of the web-based app. As an example, Figure 2-10 shows the expected averaged degree of heat stress for sheep in Cameroon for the period 2070-2098 projected with the RCP 8.5.

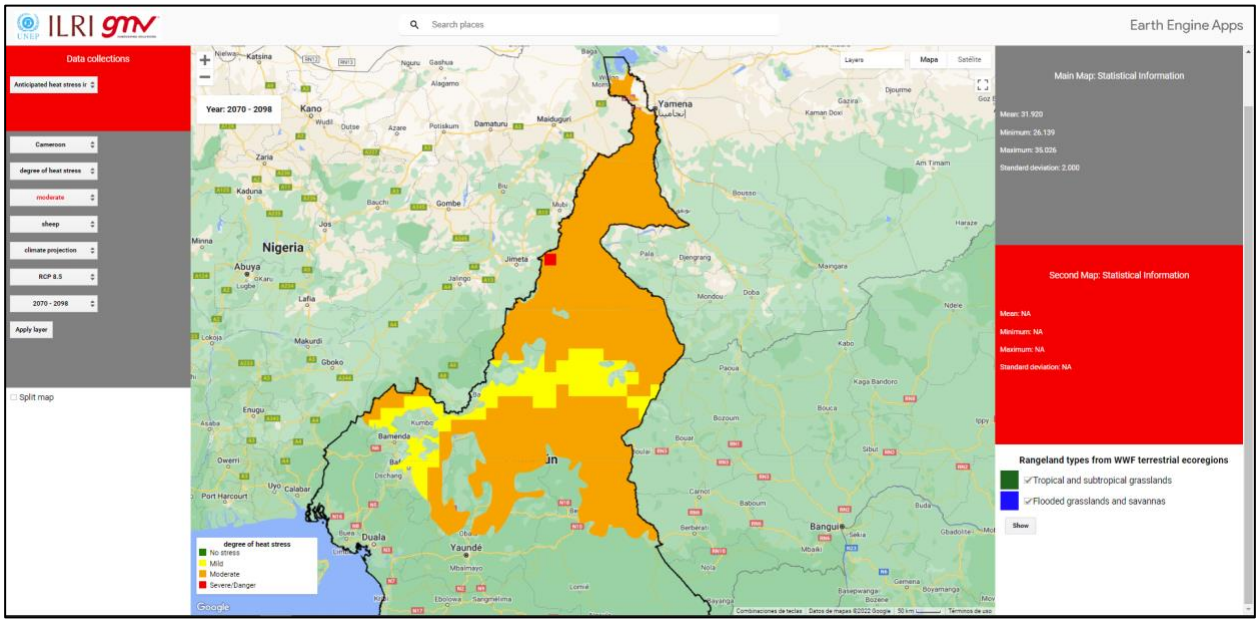

Figure 2-10 Snapshot of the anticipated degree of heat stress in livestock within the web-app.

2.4.2. AVAILABLE FEATURES

For each country in Africa, users can select any year from 1950 to 2021 in the historic analysis, and the projected periods 2006-2029, 2030-2049, 2050-2069, and 2069-2098, in the analysis of the anticipated heat stress in livestock.

In the data collection of anticipated heat stress in livestock users, in addition, should select one of the multi-gas emission scenarios, namely RCP 2.6 or RCP 8.5.

The RCP 2.6 emission pathway is representative for scenarios in the literature leading to very low greenhouse gas concentration levels. The RCP 2.6 is known as "Low emissions". This future would require: Low energy intensity, CO2 emissions stay at today’s level until 2020, then decline and become negative in 2100, a world population of 9 billion by year 2100, declining use of oil, and methane emissions reduced by 40 per cent.

RCP 8.5's radiative forcing levels by the end of 2100 are around 8.5 W/m2 under our 'best-estimate' set of model parameters with forcing levels increasing further thereafter-up to 12 W/m2 by 2250, when concentrations stabilize. This RCP is consistent with a future with no policy changes to reduce emissions. The RCP 8.5 is known as "High emissions". This future is consistent with: Rapid increase in methane emissions, heavy reliance on fossil fuels, high energy intensity,

a world population of 12 billion by 2100, and increased use of croplands and grassland which is driven by an increase in population.

After selecting the year or the period, one of the following analyses should be chosen:

- Degree of heat stress
    - Derived from the computed THI values and tailored to livestock species
- Consecutive days
    - Number of consecutive days of THI values within a certain degree of heat stress category tailored to livestock species
- Frequency of occurrence (%)
    - Frequency of days within a year of THI values within a certain degree of heat stress category tailored to livestock species
- Heat stress risk index
    - Index providing information on the heat stress risk of livestock. The risk (ranging from no risk to low risk, medium risk, and high risk) is computed as weighted average of the heat stress index values normalized by the livestock species density in the country. The livestock densities for cattle, sheep, and goats are obtained from the FAO's Gridded Livestock of the World for 2015 (GLW 4). This dataset provides the global distribution of several livestock species in 2015 expressed in total number of sheep per pixel (5 min of arc).

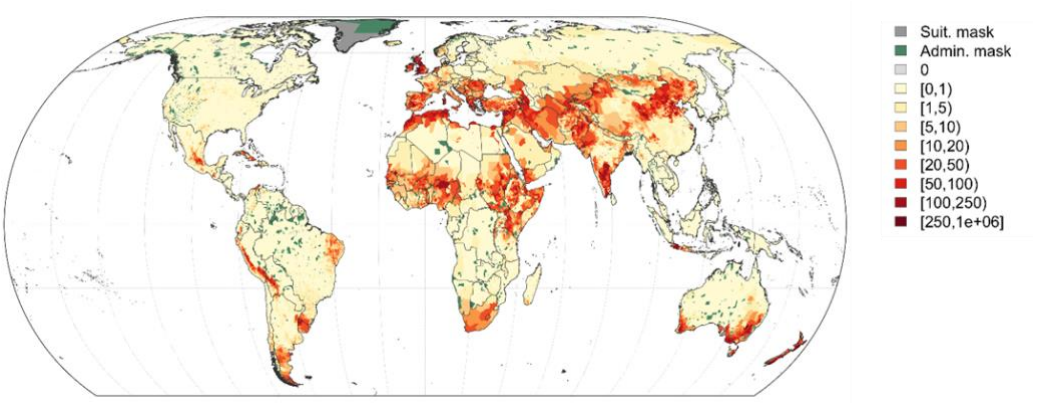

Figure 2-11 Areal-weighted sheep numbers per pixel from Gilbert et al., 2018. Note that this map corresponds to the GLW 3.

In the "Anticipated heat stress in livestock" data collection, the analyses "Consecutive days" and "Frequency of occurrence" present the following scenarios:

- Climate projection
- Difference with baseline

Climate projection presents the results derived from the projection selected (RCP + period). The difference with baseline compares the values of those indicators in the CORDEX reference period against the values in the projected period selected.

In both, anticipated and historic collections, the analyses "Consecutive days" and "Frequency of occurrence", need the user to also select the degree of heat stress of interest for the analysis.

The following option to be selected is the livestock species. Three types are available: cattle, sheep, and goats. Note that this choice is disabled for the analysis heat stress risk index, because the livestock density per country is used to weight the heat stress values.

Finally, by pressing “Apply layer”, the heat stress data is loaded for that year and country, and the results for the selected analysis are mapped. Note that the information is only shown over the rangeland systems present in Africa, as described in section 2.1, and over the areas where FAO identified livestock species (according to GLW 4) in the heat stress risk index analysis. The maximum, minimum, mean and standard deviation values of the indicator selected computed over the rangelands is shown in the right top panels.

Rangeland systems present in the country are shown in the right bottom panel. To visualize them users should press “Show” button, this will overlay a semitransparent mask over the heat stress results. Selecting and deselecting the rangeland layers will show or hide them. The statistics can be customized per rangeland type, to do so the user must select the rangeland systems of interest and press “Apply layer” in the left panel. The web-app will automatically recalculate the areas for land cover classes only over the selected rangeland types.

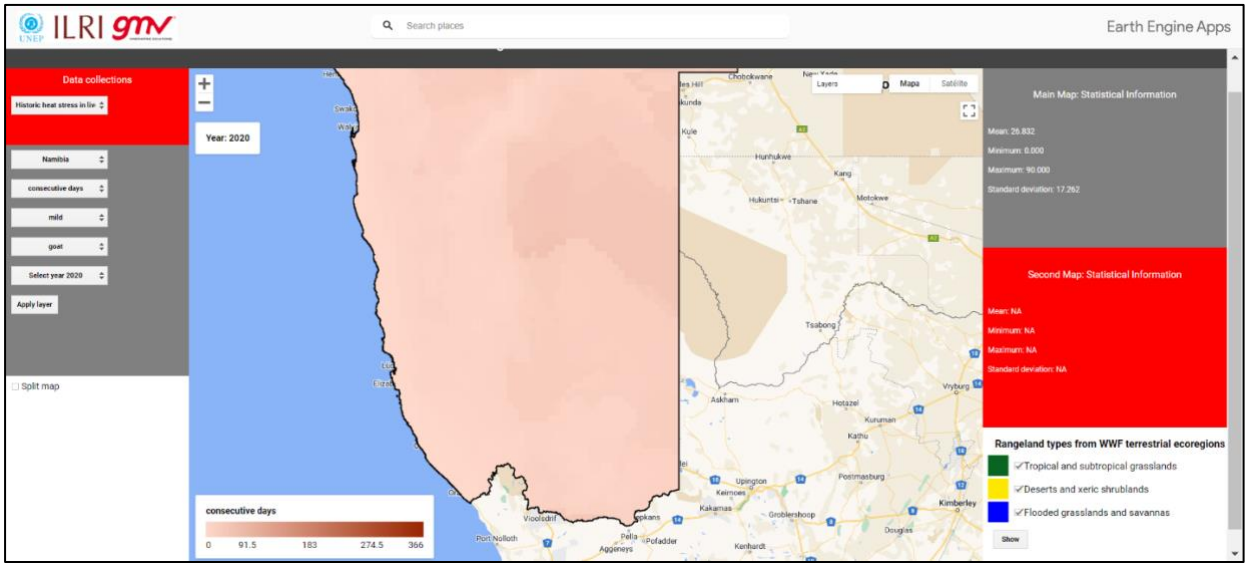

Figure 2-12 Snapshot of the web-based app showing the consecutive days of mild degree of heat stress for goat in Namibia during 2020.

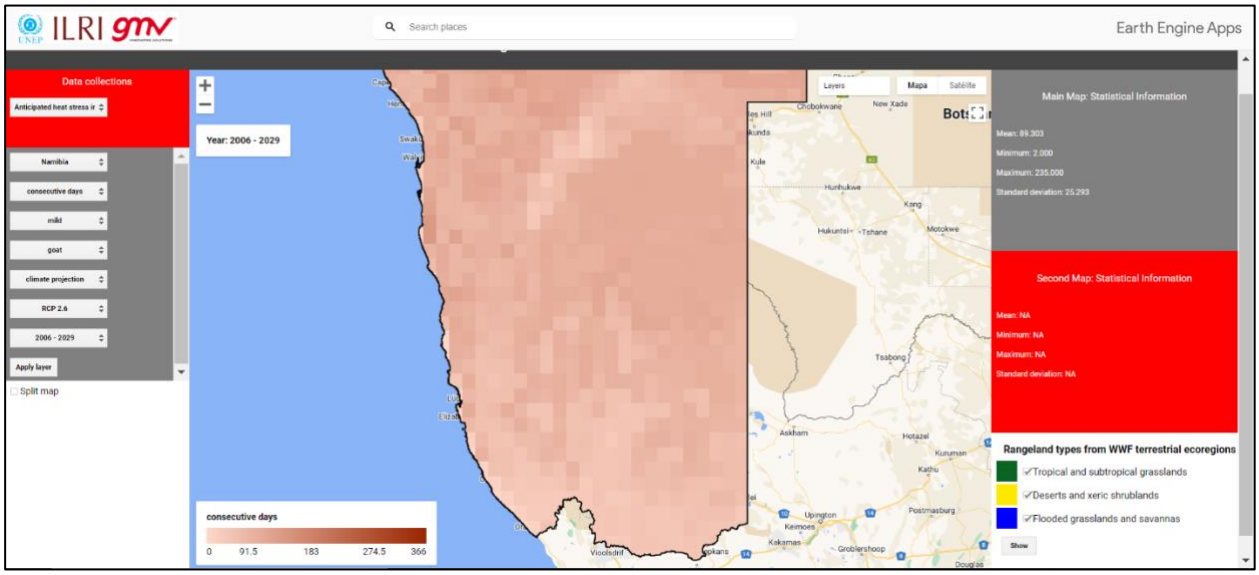

Figure 2-13 Snapshot of the web-based app showing the consecutive days of mild degree of heat stress for goat in Namibia expected in the period 2006-2029 under the RCP 2.6.

The app allows to intercompare results for different years and livestock species. To access to this functionality the user must select the “Split map” option, below the left panel. Then, select the country, the first year, the heat stress degree, and the livestock species in the top left panel, and “Apply layer” to show the first map, and the second year, the heat stress degree, and the livestock species of study in the bottom left panel, and “Apply layer” to show second map.

Figure 2-14 shows an example of the frequency of occurrence of heat stress over Niger during 1950 and 2000 presented simultaneously. Figure 2-15 shows an example of the heat stress risk index over Niger for the periods 2030-2049 and 2070-2098 under the RCP 8.5 presented simultaneously. In both cases, the horizontal scroll line allows scrolling left and right to quickly analyze changes in the two years/ periods selected. The mean, standard deviation, max and min statistics of the two maps are shown in the right statistical panels. In the split mode, user can also select certain rangeland layers are recalculate the coverage statistics by pressing the corresponding “Apply layer” buttons in the left panels.

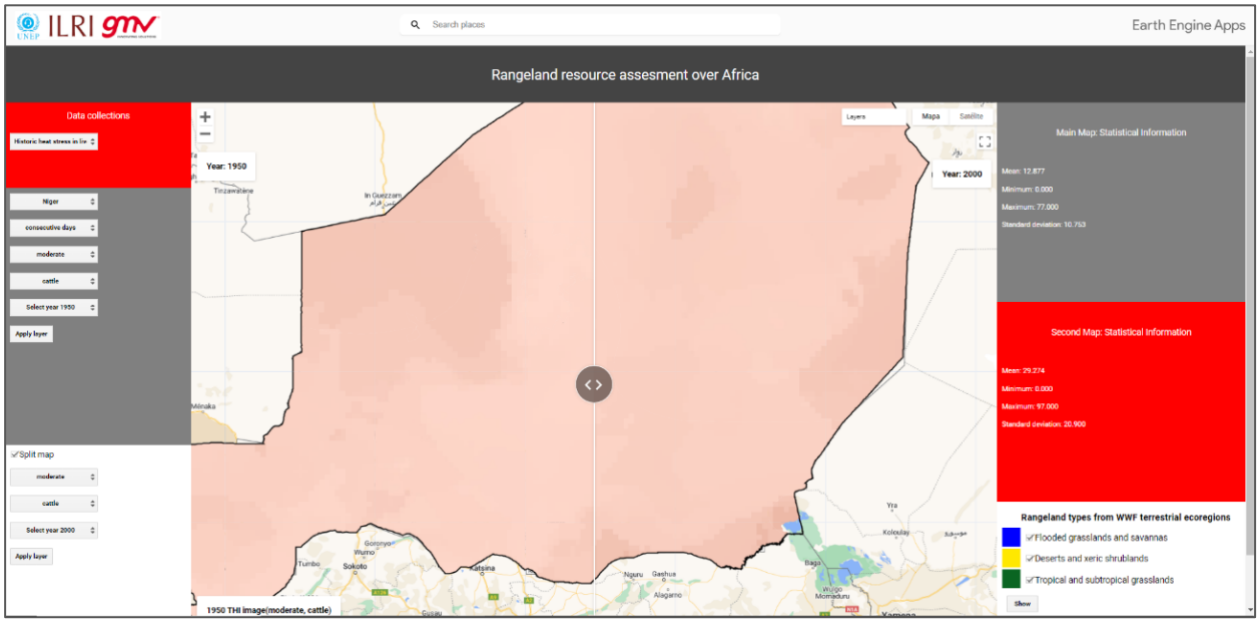

Figure 2-14 Snapshot of the historic heat stress in livestock product in the split mode.

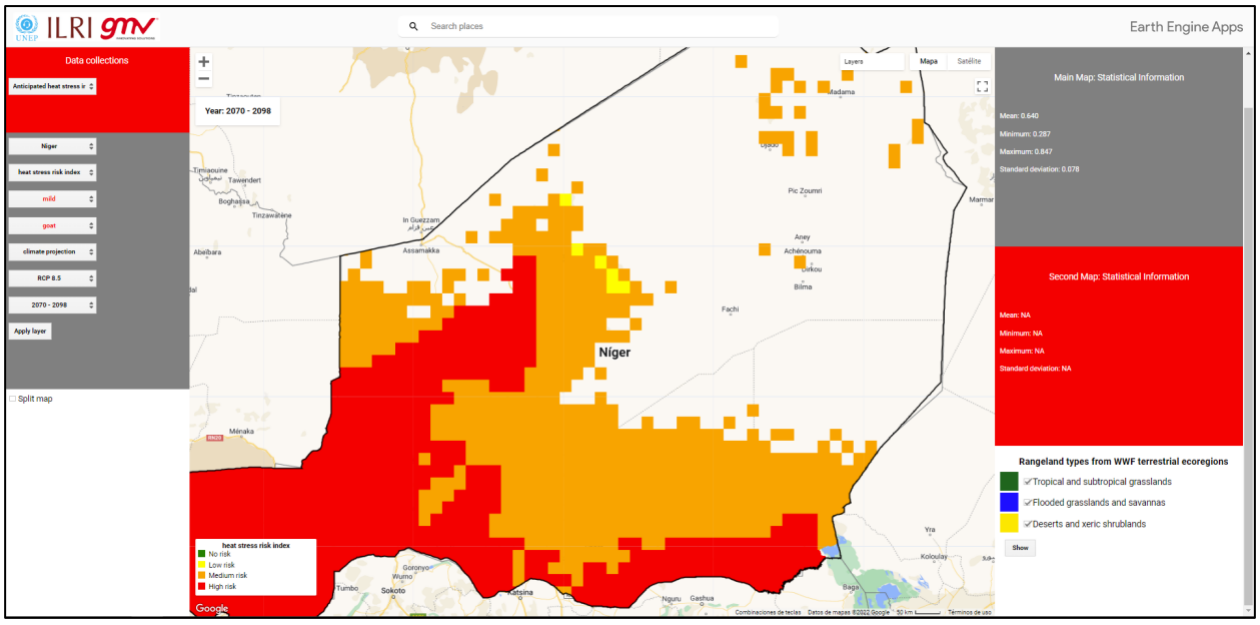

Figure 2-15 Snapshot of the anticipated heat stress in livestock product in the split mode.

2.5. NET PRIMARY PRODUCTIVITY

The net primary productivity (NPP) represents the ability of the vegetation to fix atmospheric carbon as biomass and is therefore a substantial indicator of biomass dynamics in rangelands, fluctuation based on grazing, management, climate change, and human interference such as land-use change.

NPP is obtained from the product MOD17A3H Version 6. This an Earth Observation product from the Moderate Resolution Imaging Spectroradiometer (MODIS) instrument on-board the Terra satellite. This product provides information about annual NPP, in kg C/m2, at 500m pixel resolution from 2000 to 2021. The full timeseries is included in the web-based app.

The MODIS NPP follows the logic of John L. Monteith (1972) that suggests that the NPP of well-watered and fertilized annual crop plants was linearly related to the amount of solar energy the plants absorbed over a growing season. This logic combined the meteorological constraint of available sunlight reaching a site with the ecological constraint of the amount of leaf area absorbing the solar energy, while avoiding many complexities of canopy micrometeorology and carbon balance theory. Measures of absorbed photosynthetically active radiation (APAR) integrate the geographic and seasonal variability of day length and potential incident radiation with daily cloud cover and aerosol attenuation of sunlight. In addition, APAR implicitly quantifies the amount of leafy canopy that is displayed to absorb radiation (i.e., LAI). A conversion efficiency, ε, translates APAR (in energy units) to final tissue growth, or NPP (in biomass). GPP is the initial daily total of photosynthesis, and daily net photosynthesis (PSNnet) subtracts leaf and fine-root respiration over a 24-hour day. NPP is the annual sum of daily net PSN minus the cost of growth and maintenance of living cells in permanent woody tissue.

The NPP is an input for the calculation of the Human Appropriation of Net Primary Productivity (HANPP), but it has enough relevance for research activities to include it in the web-based app as an independent product. HANPP is used to measure the impact of human land use on the natural potential to provide NPP.

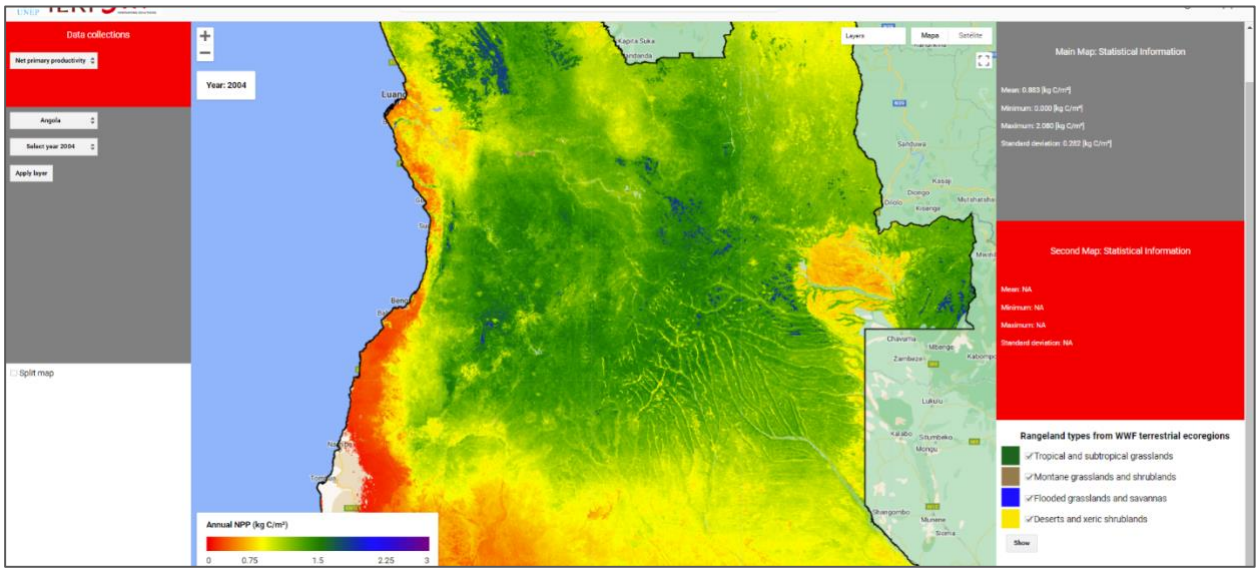

Figure 2-16 Snapshot of the net primary productivity product within the web-app.

2.5.1. AVAILABLE FEATURES

The NPP maps are presented in the platform as shown in the example depicted in Figure 2-16.

Users can select any year from 2000 to 2021, and the country of interest. After pressing “Apply layer”, the NPP for that year and country are mapped. Note that the information is only available over the rangeland systems present in Africa as described in section 2.1. The minimum, maximum, standard deviation and mean NPP values for the country are computed and shown in the right top panels.

Rangeland systems present in the country are shown in the right bottom panel. To visualize them users should press “Show” button, this will overlay a semitransparent mask over the NPP map. Selecting and deselecting the rangeland layers will show or hide them. The max, min, mean and standard deviation NPP statistics can be calculated per rangeland type, to do so the user must select the rangeland systems of interest and press “Apply layer” in the left panel. The web-app

will automatically recalculate the areas for land cover classes only over the selected rangeland types.

To intercompare results for different years, the user must select the “Split map” option, below the left panel. Then, select the country and the first year in the top left panel, and “Apply layer” to show the first map, and the second year of study in the bottom left panel, and “Apply layer” to show second map.

Figure 2-17 shows an example of NPP maps over Botswana for 2010 and 2006 presented simultaneously. The horizontal scroll line allows scrolling left and right to quickly analyze changes in the two years selected. The NPP statistics of the two maps are shown in the right statistical panels. In the split mode, user can also select certain rangeland layers are recalculate the NPP statistics by pressing the corresponding “Apply layer” buttons in the left panels.

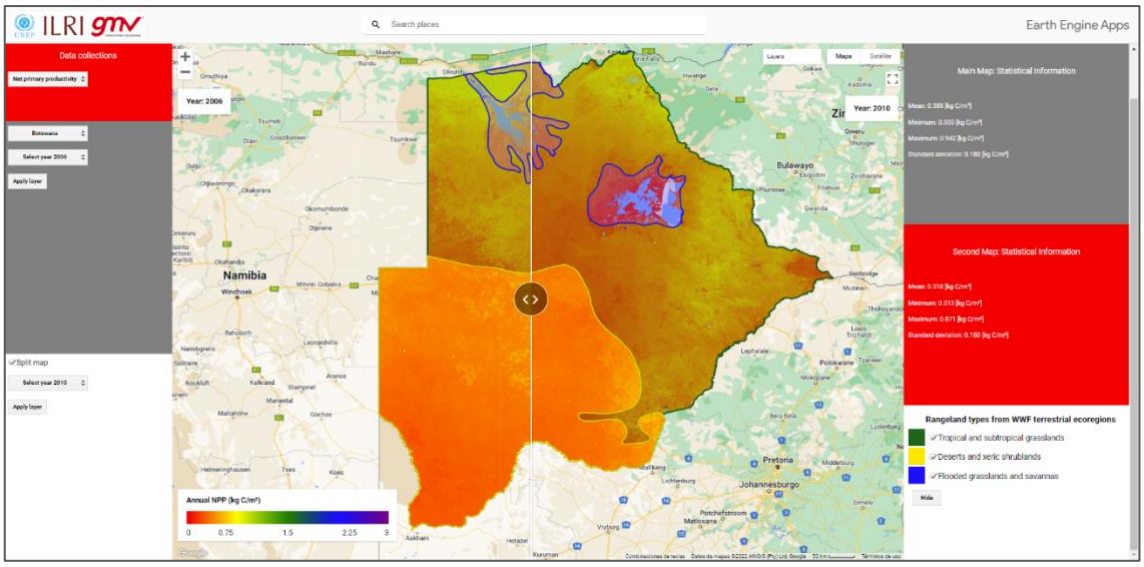

Figure 2-17 Snapshot of the NPP product in the split mode.

2.6. HUMAN APPROPRIATION OF NET PRIMARY PRODUCTIVITY

As presented in Section 2.5, NPP is the net amount of carbon assimilated in a given period by the vegetation. All organisms (e.g., all species of animals including humans) depend on the primary production of plants as an essential basis of their livelihood.

At global level, humans use a disproportionate and growing component of NPP. NPP is indeed the primary source upon which humans rely to feed themselves and their domesticated animals. According to the World Atlas of Desertification, the diversion of products of these biological processes to sustain human populations can have profound impacts on the structure and functioning of global ecosystems. This may result in ecosystem perturbations that can exceed their natural variability and dynamics and result in persistent weakening of ecosystem functioning and finally a transformation of existing ecosystems into something quite different. These transformations or state changes may result in decreased economic and ecological value. Increasing amounts of NPP claimed by humans also means that less biomass remains for sustaining other species and maintaining ecosystems now and into the future.

The proportion of NPP consumed directly by mankind land use is known as Human Appropriation of Net Primary Productivity (HANPP). HANPP characterizes the extent to which anthropogenic land conversion and biomass harvest alter the natural capacity of primary biomass production (NPP_0) of “undisturbed” terrestrial ecosystems under current climate conditions.

Considering HANPP (Haberl et al., 2007) as the combined effect of harvest and productivity changes induced by land use on the availability of NPP in ecosystems, HANPP is calculated as the difference between the NPP_0, i.e., the plant cover that would prevail in the absence of human

$$HANPP = NPP_0 - NPP_t$$

intervention and the fraction of NPP remaining in ecosystems after harvest (NPP_t).

NPP_t is calculated by subtracting the amount of NPP harvested (NPP_h) from the actual NPP actual

$$NPP_t = NPP_{act} - NPP_h$$

under current land use (NPP_{act}).

HANPP, thus, can be estimated from:

$$HANPP = NPP_0 - (NPP_{act} - NPP_h)$$

The HANPP index has been calculated to assess the impact of the human activities in the African rangeland ecosystems. The different NPP variables have been estimated as follows:

- NPP_0 is assumed to prevail in the absence of land use but with current climate. It is estimated from the model LPJmL ("Lund-Potsdam-Jena managed Land").
    - The LPJmL model is a Dynamic Global Vegetation Model (DGVM), which was designed to simulate the global terrestrial carbon cycle and the response of carbon and vegetation patterns under climate change.
    - The model results come from the ISIMIP2a simulation round. The Inter-Sectoral Impact Model Intercomparison Project (ISIMIP) offers a framework for consistently projecting the impacts of climate change across affected sectors and spatial scales. The ISIMIP2a simulation round focused on quantifying the impacts of GCM-derived historical and CMIP5 (Coupled Model Intercomparison Project Phase 5) projected climate change relative to a pre-industrial control. Therefore, this is consistent with the CORDEX data employed in the heat stress on livestock analysis.
    - The historical period (historical climate scenario) and natural socio-economic scenario (no direct human influence) is selected to obtain the NPP_0. The historical period for this round run from 2000 to 2012.
- NPP_{act}, the NPP of the actual vegetation is obtained from satellite data as described in Section 2.5.
- NPP_h: The NNP harvested is derived from FAOSTAT data.
    - NPP_h has been computed for grazing activities, either directly for grazing or indirectly from mowing or harvest for hay or silage.
    - To compute the amount of biomass consumed by ruminants, we established a feed balance for each country and estimated the demand for grazing as the difference between the supply of commercial feed, fodder crops, as reported in

FAO statistics, and crop residues, using an averaged harvest factor over the crop production, and the aggregate feed demand of livestock following Table 2-5.

Table 2-5 Species-specific daily feed intake (kg DM/head/day) from Haberl et al., 2007

Livestock	Nord Africa	Sub-Saharan Africa
Cattle	6.8	6.7
Sheep and goats	1.0	1.1

- To compute the amount of biomass produced by planted forage or green fodder crops, we estimated production from FAO statistics.
- NPP_h from croplands or forestry activities is not considered. However, it must be noted that the WWF ecoregions selected as rangelands consider many different land cover classes (e.g., forest, croplands, etc.).

The values of the NPP variables are averaged in 3-year periods starting from 2000 until 2012 (2000 – 2002, 2003 – 2005, 2006 – 2008, 2009 – 2012), and therefore the HANPP is estimated for those periods.

This dataset is not included in the web-based app as considered yet experimental.

3. ANALYSIS OVER SENEGAL AND ETHIOPIA

The objective of this chapter is to showcase the analyses on rangelands that can be done using the datasets and tools from the web-based app. Two countries, Senegal, and Ethiopia have been chosen to present examples of the different analyses on land cover changes on rangeland systems, on the impact of climate change in the livestock productivity, and on the human impact on rangelands ecosystems that allows our new application.

3.1. SENEGAL

(From FAO, World Bank, SustainSahel, 2022).

Located in the westernmost part of the African continent, Senegal is bordered by Mauritania, Mali, Guinea, and Guinea-Bissau. Senegal enjoys a dry tropical climate and has a population of 16.7 million people and a population density of 87 people per km2.

The northern part of the country is characterized by an arid Sahelian climate, with higher temperatures and an annual rainfall average of about 360 mm, a strong contrast to the southern region of Casamance, where rainfall averages between 1,200 and 1,500 mm annually.

Around 75% of the population is engaged in agriculture, with the main crops being millet, sorghum, rice, peanuts, cowpeas, and cotton. Livestock production is more important in the arid north, where it is the main economic activity. The country's livestock population includes approximately 3 million cattle and 8.7 million small ruminants (sheep and goats). Senegal's GDP in 2020 stood at $24.9 billion in current terms. Its per capita gross national income (GNI) was $1,430 in 2020, making it a lower-middle-income country. The country ranks 170 of 191 in the human development index report of 2021, with a score of 0.511, indicating a low human development rating for Senegal.

3.1.1. RANGELANDS DEGRADATION AND ENVIRONMENTAL THREATS/CLIMATE HAZARDS

The analysis of the existing land covers in Senegal's rangeland systems through the platform provides very useful information to analyse the current situation.

According to the information from the WWF Terrestrial ecoregions, only one rangeland system is present in the country: Tropical and subtropical grasslands. This rangeland covers almost all the country, only the coastal area of the Casamance River is excluded.

The land cover classes present in the rangeland and the coverage statistics obtained for 1992 and 2020 are displayed in Figure 3-1. For visualization purposes, the cover extents for 2020 are provided in the list below.

Cropland, rainfed

46083 Km2

Cropland, irrigated or post-flooding

2629 Km2

Mosaic cropland (>50%) / natural vegetation (tree, shrub, herbaceous cover) (<50%)

9217 Km2

Mosaic natural vegetation (tree, shrub, herbaceous cover) (>50%) / cropland (<50%)

4665 Km2

Tree cover, broadleaved, deciduous, closed to open (>15%)

30671 Km2

Mosaic tree and shrub (>50%) / herbaceous cover (<50%)
21127 Km2
Mosaic herbaceous cover (>50%) / tree and shrub (<50%)
76 Km2
Shrubland
59806 Km2
Grassland
11349 Km2
Sparse vegetation (tree, shrub, herbaceous cover) (<15%)
394 Km2
Tree cover, flooded, fresh or brakish water
420 Km2
Tree cover, flooded, saline water
1299 Km2
Shrub or herbaceous cover, flooded, fresh/saline/brakish water
3413 Km2
Urban areas
663 Km2
Bare areas
73 Km2
Water bodies
2660 Km2

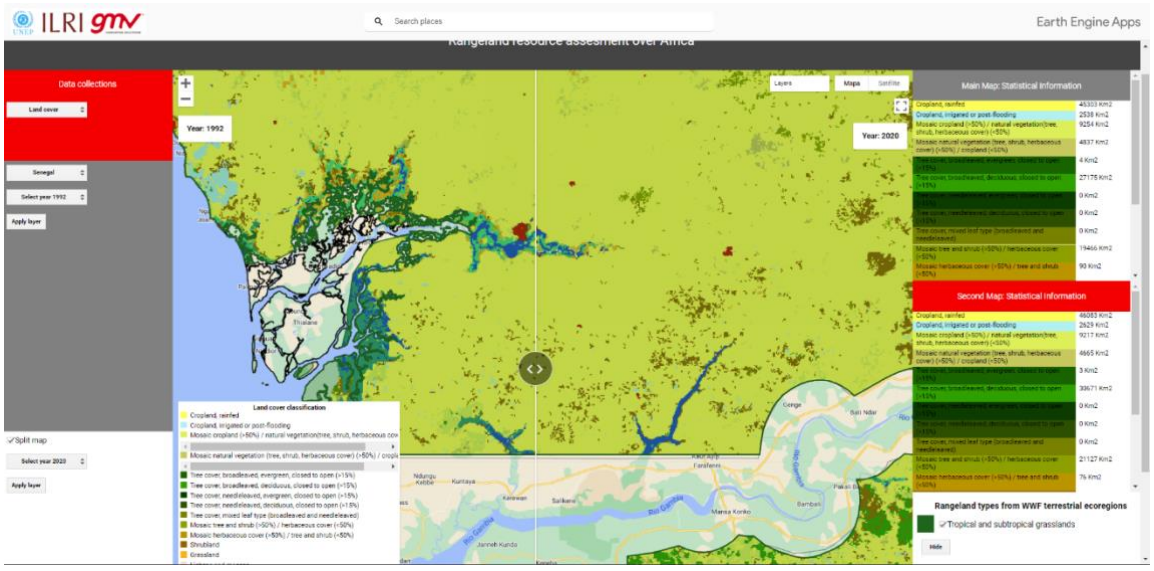

Figure 3-1 Snapshot of the land cover classes, and area statistics over Senegal displayed in the platform for 1992 and 2020 with the split mode.

Comparing the land cover situation of 1992 and 2020 in the rangeland areas of Senegal, the rainfed cropland areas changed from 45,000 km2 to 46,000 km2 being the second most predominant class after shrublands that changed from 64,000 km2 to 60,000 km2. The different mosaics of vegetation covered 33,000 km2 in 1992 and 35,000 km2 in 2020, while grasslands

decreased from 13,000 km to 11,000 km2. The degradation of the rangeland system in Senegal with the decrease of pasturelands and the increase of the cropland areas is very significant in the period.

The transformation processes of these grazing areas can also be studied in the platform with the land cover transition collection. Figure 3-2 shows the transitions of land cover between 1992 and 2002. The crop expansion in original grazing areas in most notably in the region of Louga, but Saint-louis in Northeast and Kolda near Gambia are experienced significant reduction in grazing areas.

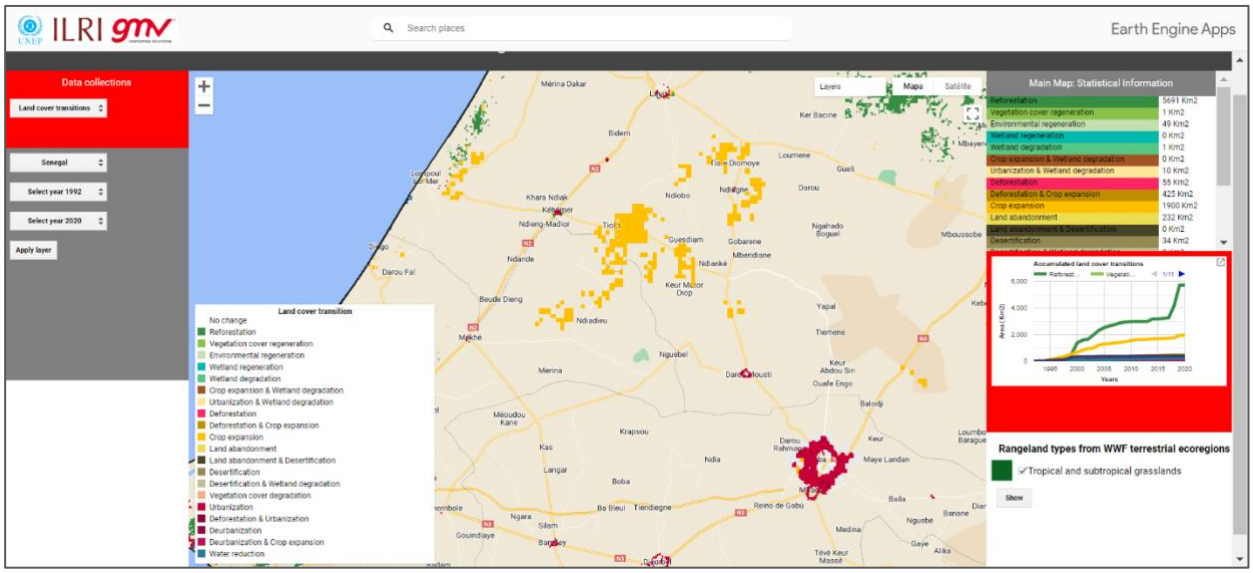

Figure 3-2 Snapshot of the land cover transitions and area statistics between 1992 and 2020 displayed in the platform.

The web system also allows to analyse the land cover dynamic trends over the different rangelands in the country. For Senegal's rangeland Tropical and subtropical grasslands, Figure 3-3 provides the accumulated area of the land cover transitions from 1992 to 2020.

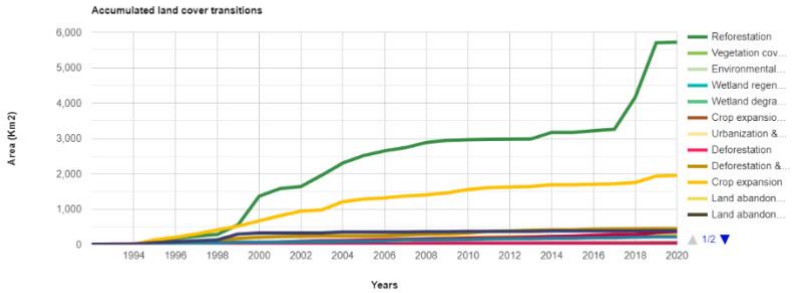

Figure 3-3 Timeseries of accumulated land cover transitions in Senegal over the tropical and subtropical grasslands.

The annual change normalized by the total area of the rangeland system is shown in Figure 3-4. The information to create these graphics is available in the platform, but the functionality to create automatically the annual graphs is not yet available in the system.

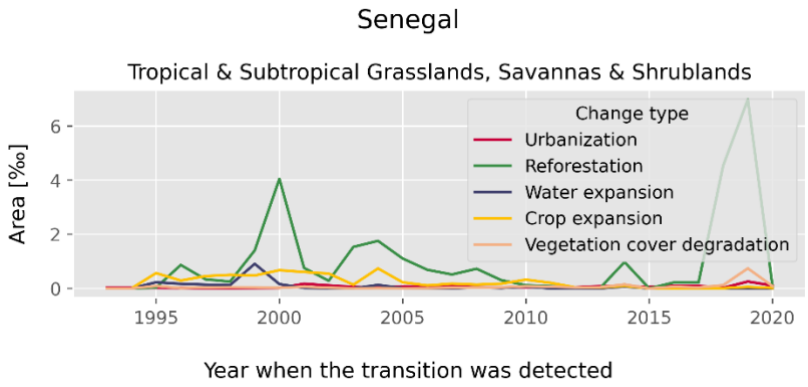

Figure 3-4 Timeseries of annual land cover change in Senegal over the tropical and subtropical grasslands. Not yet available in the web-based app.

3.1.2. NEXUS BETWEEN RANGELANDS, ONE HEALTH, AND SUSTAINABLE FOOD SYSTEMS

To analyse the nexus between rangelands and the food systems, the web-based app has different analyses and functionalities available.

Figure 3-5, Figure 3-6 and Figure 3-7 show the heat stress in livestock over the Senegal rangeland systems for cattle, goats, and sheep for two different timestamps: 1950 and 2021. For all three species an increase of the degree of heat stress is found. That can be qualitatively observed in the geospatial maps by comparing the results (with the scroll bar) in the coastal areas, with some areas changing from “no stress” to “mild stress” for the three species, or with the change from “mild stress” to “moderate stress” in sheep over the north-eastern rangelands. In the right panels the statistics allow preparing a quantitative assessment by comparing the max, min, standard deviation, and mean values over the country.

The analysis on sheep livestock can be further extend using the analysis of consecutive days and frequency of occurrence. Figure 3-8 shows the frequency of occurrence during 1950 and 2021 of the moderate degree of heat stress in sheep for Senegal. Almost 60% of days in 2021 with moderate heat stress in the areas with the highest percentage of occurrence compared to 40% of days during 1950. The mean value over all the rangeland areas also increased from 26% to 36%.

The consecutive days of severe heat stress are depicted in Figure 3-9. In 1950, the THI index applied to sheep does not show a single day with severe degree in heat stress, the worst situation was 69 consecutive days in moderate heat stress. However, in 2021, the maximum consecutive days under moderate heat stress moved up to 107 and start appearing areas with severe heat stress.

Figure 3-10 shows the results for the projected climate under RCP 8.5 in Senegal. In particular, the figure presents the difference of consecutive days under severe heat stress when compared the projected scenario against the baseline historic period. A maximum increase of 239 days is observed, with a minimum of 5 days. The geospatial analysis shows mild changes near the coast with the most extreme consequences over the centre and northeast region of Senegal.

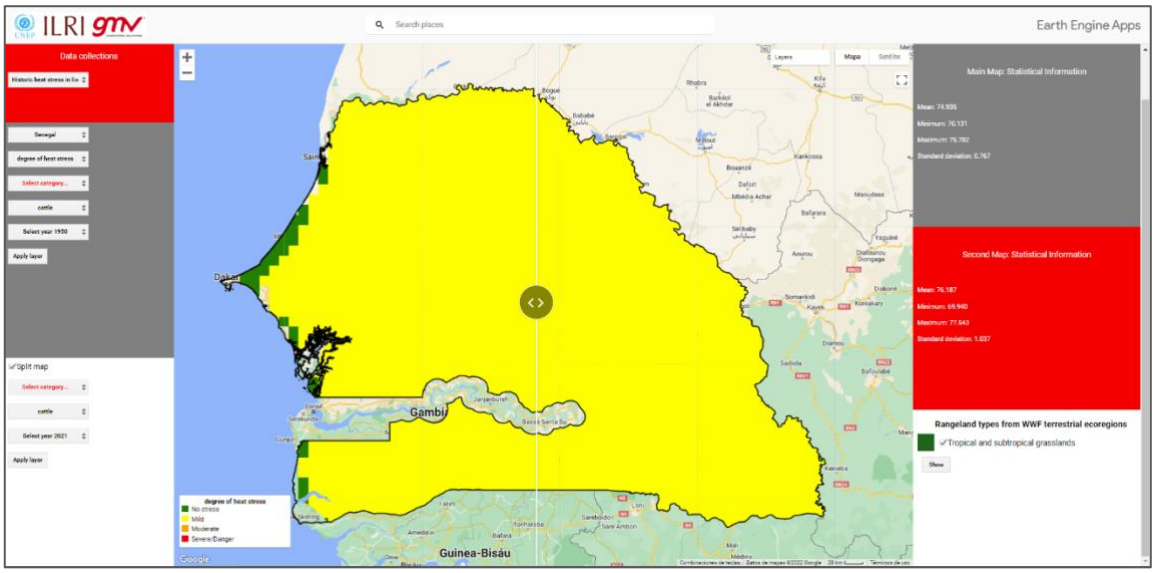

Figure 3-5 Snapshot of the differences in cattle heat stress for Senegal (1950-2021).

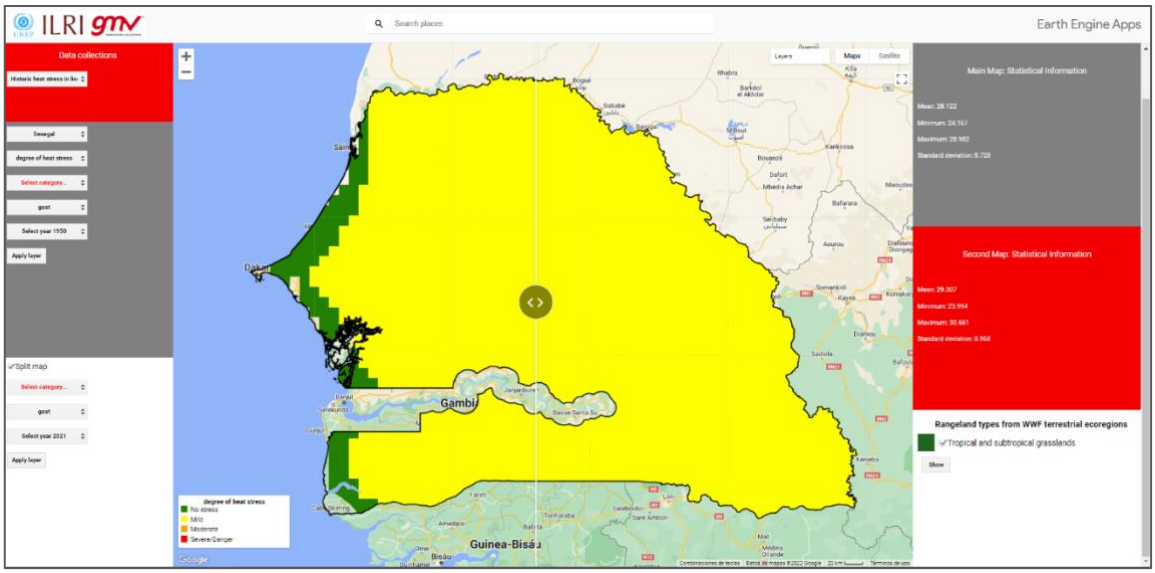

Figure 3-6 Snapshot of the differences in goats heat stress for Senegal (1950-2021).

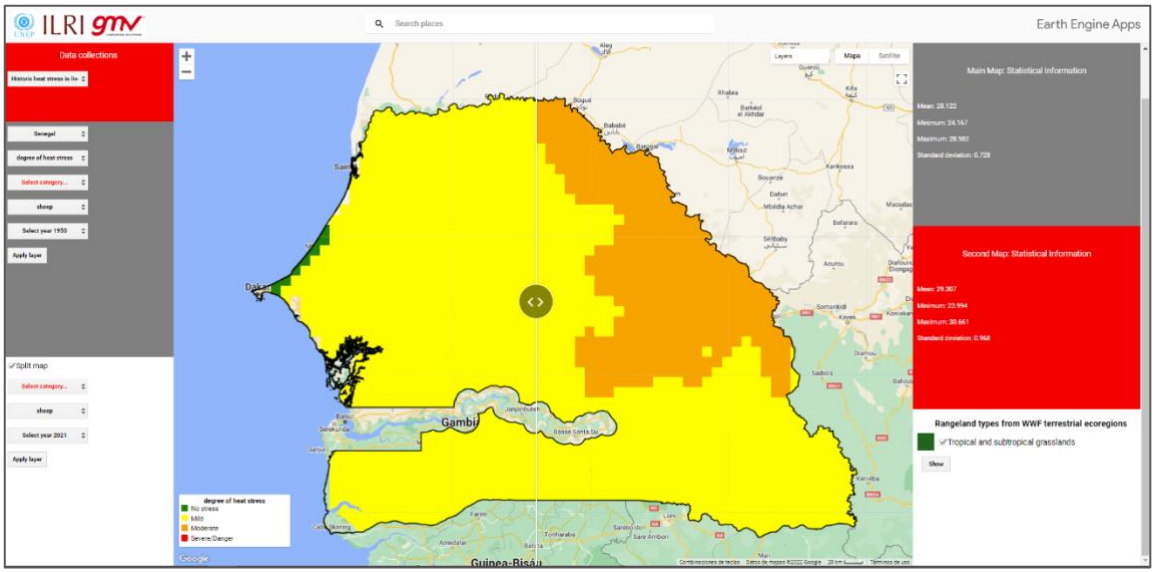

Figure 3-7 Snapshot of the differences in sheep heat stress for Senegal (1950-2021).

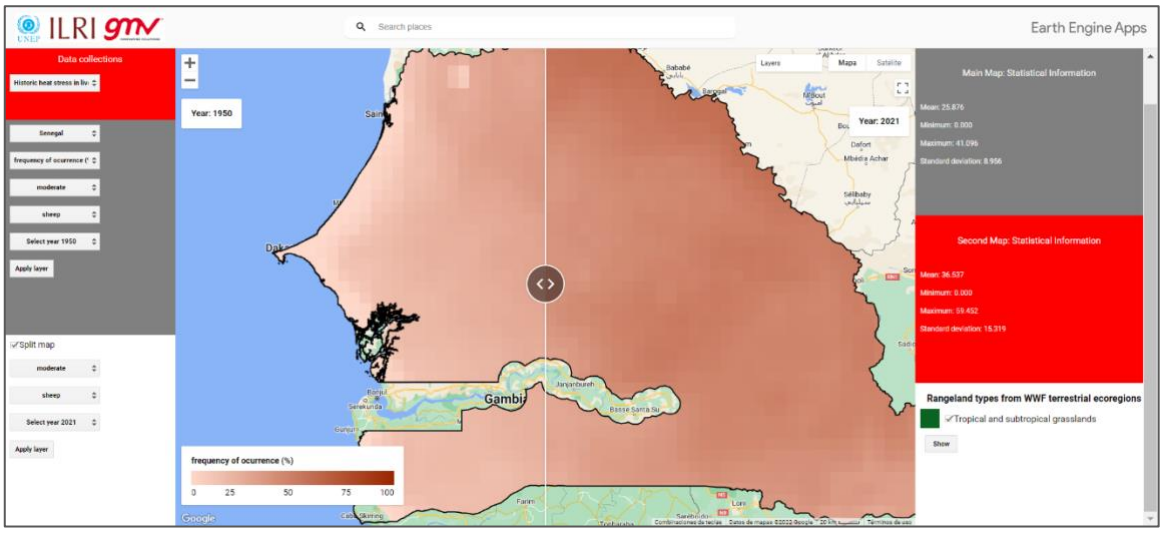

Figure 3-8 Snapshot of the differences in the frequency of occurrence of moderate heat stress in sheep for Senegal (1950-2021).

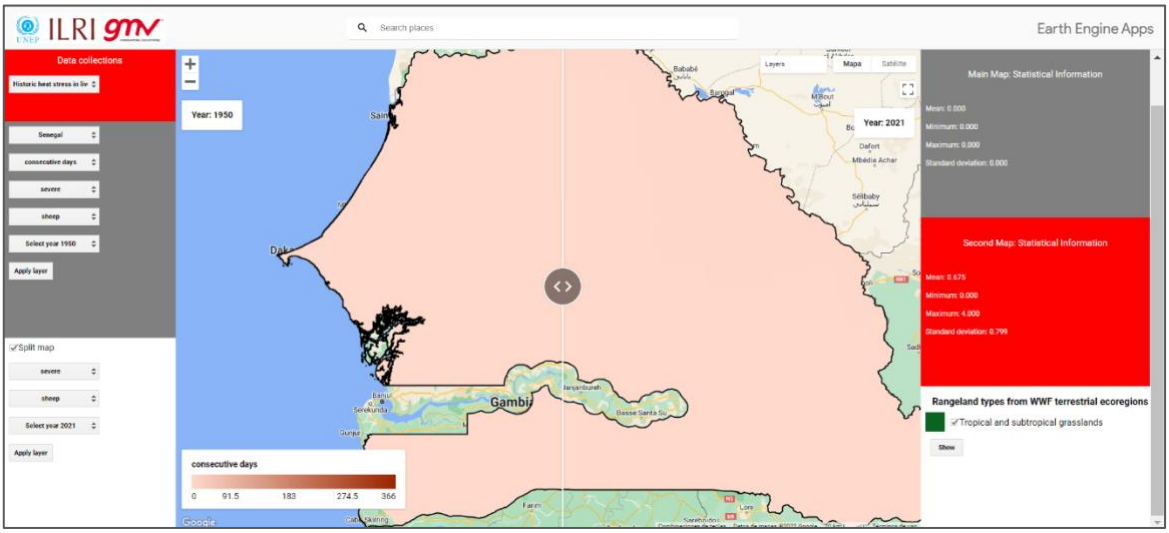

Figure 3-9 Snapshot of the differences in the consecutive days of severe heat stress in sheep for Senegal (1950-2021).

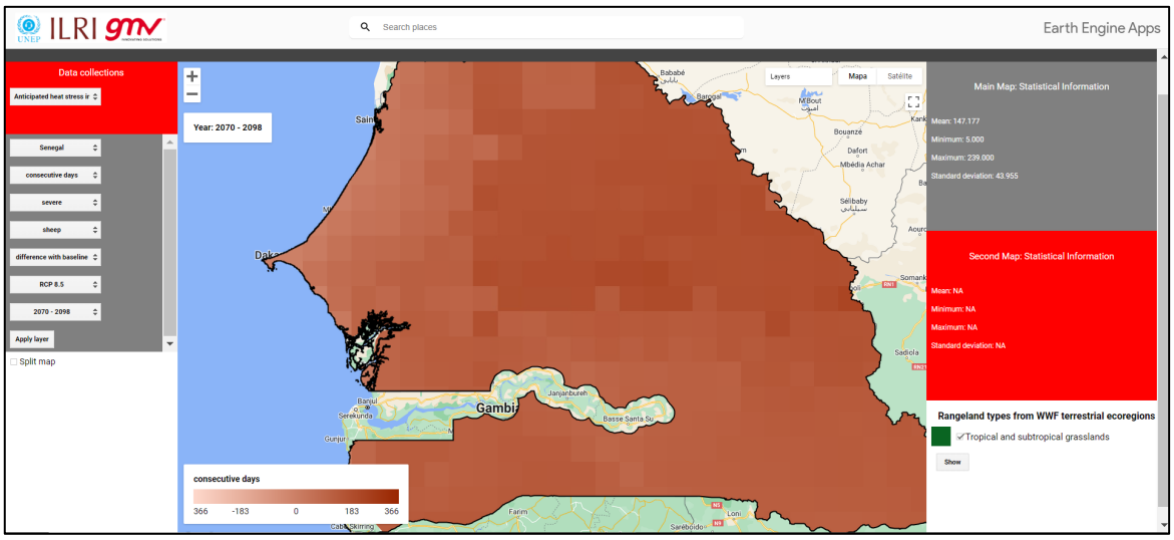

Figure 3-10 Snapshot of the differences with respect to the reference historic period in the consecutive days of severe heat stress in sheep for Senegal expected for the end of the century (2070-2098) under the RCP 8.5.

3.2. ETHIOPIA

(From FAO, World Bank, 2022).

Ethiopia, with a total area of 1.1 million km2, lies in the northeastern part of the Horn of Africa. The country is landlocked, sharing frontiers with Eritrea to the north and northeast, Djibouti to the east, Somalia to the east and southeast, Kenya to the south, and South Sudan and Sudan to the west.

Ethiopia's topographical diversity encompasses high mountains and flat-topped plateau, surrounded by lowlands, and dissected by deep gorges with rivers and rolling plains with altitudes ranging from 110 m below sea level at the Denakil Depression in the northeast to over 4,600 m above sea level in the Simien Mountains in the north. The Great East African Rift Valley divides the country.

It is estimated that 16 million ha is cultivated, and 20 million ha are permanent pastures. Water bodies cover around 744,400 ha, forest, and woodland about 4 million ha and 29 million ha respectively, while over 26 million ha are protected.

With about 117 million people (2021), Ethiopia is the second most populous nation in Africa after Nigeria, and still the fastest growing economy in the region, with 6.3% growth in FY2020/21. However, it is also one of the poorest, with a per capita gross national income of $960. Ethiopia aims to reach lower-middle-income status by 2025. The country ranks 170 of 191 in the human development index report of 2021, with a score of 0.498, indicating a low human development rating for Ethiopia.

3.2.1. RANGELANDS DEGRADATION AND ENVIRONMENTAL THREATS/CLIMATE HAZARDS

The analysis of the existing land covers in Ethiopia's rangeland systems through the new web-based app provides lot of information to analyse the current and past states of the rangelands, together with the trend.

According to the information from the WWF Terrestrial ecoregions, four rangeland types cover the country:

- Tropical and subtropical grasslands
- Deserts and xeric shrublands
- Flooded grasslands and savannas
- Montane grasslands and shrublands

The land cover classes present in the three of four rangeland systems of Ethiopia for 1992 and 2020 are displayed in Figure 3-11. Note that the land cover coverage shown in the right panels correspond to the area estimated accounting for the entire rangelands mask in the country. However, the semi-transparent layers of rangeland that overlap the land cover maps for 1992 and 2020, can be disabled or enabled to allow re-computing the coverage statistics for specific rangeland systems.

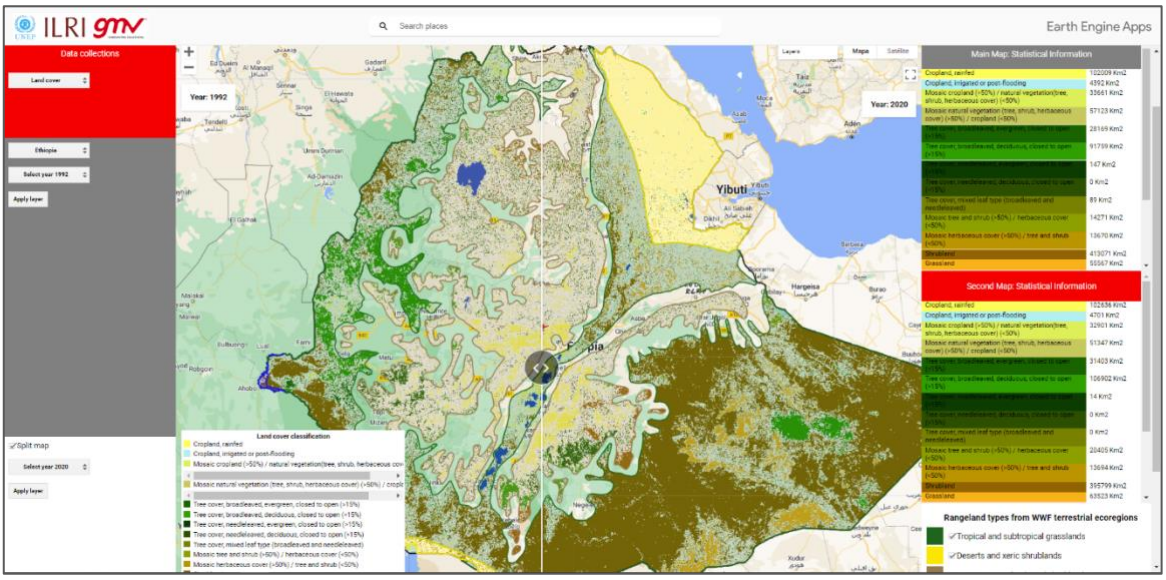

Figure 3-11 Snapshot of the land cover classes, and area statistics calculated between 1992 and 2020 over the rangeland systems in Ethiopia.

For instance, the land cover corresponding to grasslands and shrublands of the rangeland type "montane grassland and shrublands" decreases when comparing the maps of 1992 and 2020.

1992

Shrubland

43235 Km2

Grassland

410 Km2

2020

Shrubland

36777 Km2

Grassland

341 Km2

In the "Tropical and subtropical grasslands" rangeland type the situation is the opposite and the grassland land cover shows a significant increase

1992

Grassland

50381 Km2

2020

Grassland

57993 Km2

While in the "Deserts and xeric shrublands" rangeland system the land cover class shrubland shows a decrease in area, as shown in Figure 3-12.

1992

Shrubland

1637 Km2

2020

Shrubland

1489 Km2

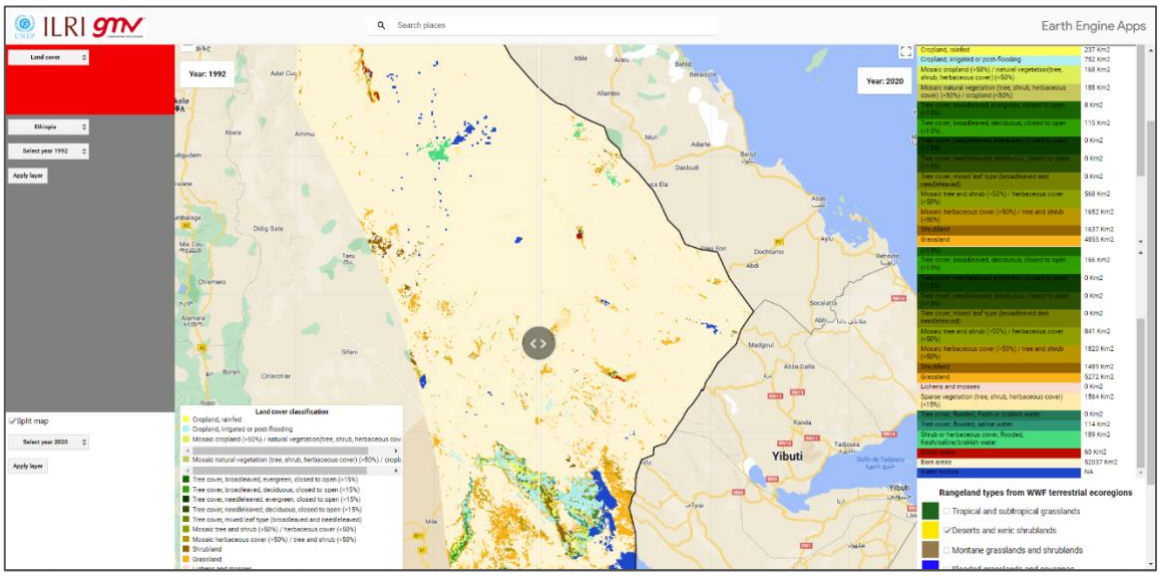

Figure 3-12 Snapshot of the land cover classes, and area statistics calculated between 1992 and 2020 over the Deserts and xeric shrublands in Ethiopia.

The land cover dynamics of the Ethiopian rangelands over the last 30 years are shown in Figure 3-13. Left plots present the accumulated area of the different transformation processes during the complete data series of C3S land cover maps for each of the rangeland types, while right plots correspond to the annual land cover transitions relative to the total area of each rangeland type (in 1/1000).

The most relevant dynamics at country level in terms of extent of changes are shown in Figure 3-13, for every rangeland type. Those transitions might not be the most relevant changes for each of the rangeland systems, but we kept the same in all the plots for visualization purposes. The platform actually presents all existing transitions for a given rangelands type.

Crop expansion processes, deforestation/ reforestation and degradation of wetlands are the most significant dynamics at country level. It should be noted that some of the transitions might be overestimated or underestimated, because the transition matrix combines multiple land cover classes and many of these classes are already a mosaic of covers. For a detailed analysis is recommended to study the changes with the original land cover classes instead of relying in the results from the transition product.

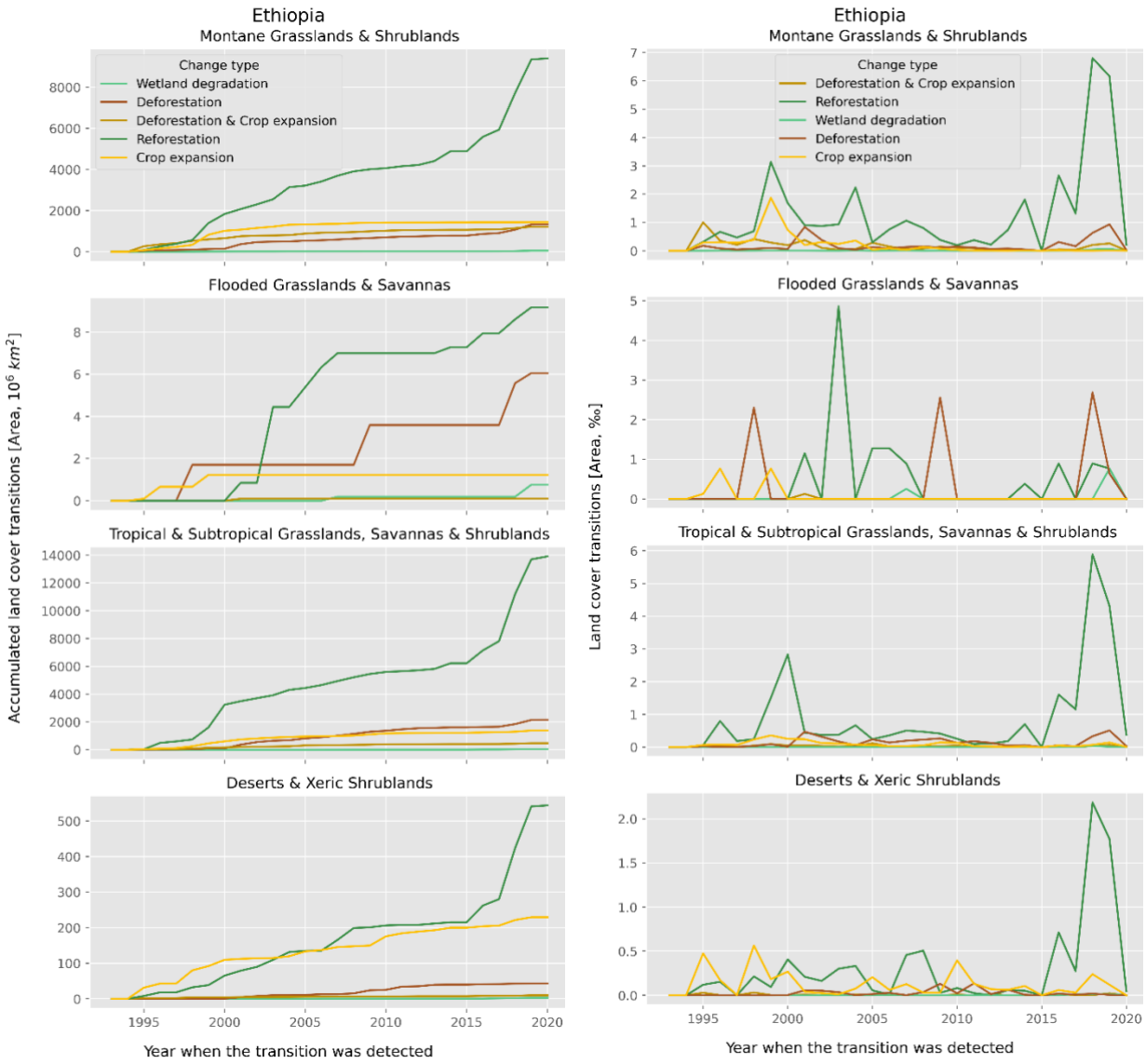

Figure 3-13 Timeseries of accumulated annual land cover transitions (left) and annual relative land cover changes (right) in Ethiopia over existing rangeland systems.

3.2.2. NEXUS BETWEEN RANGELANDS, ONE HEALTH, AND SUSTAINABLE FOOD SYSTEMS

To intercompare the heat stress in livestock obtained for different countries or for different regions over the same country, the THI index used to estimate the stress must be normalized by the density of livestock species. The index is calculated per livestock species and the distributions of species change geographically, therefore without the normalization the geospatial comparison of risk is not realistic. This new index can be interpreted as the risk of being the total livestock under significant heat stress. This dataset is not yet included in the web-based app, but it is expected to be incorporated in the data catalogue by the end of 2022.

Figure 3-14 presents the heat stress risk for each of the seasons in 2021 in Ethiopia. Considering the three livestock species analysed (cattle, goats, and sheep), the livestock being grazed in the Northeast region of Ethiopia is the most affected by the current climate conditions.

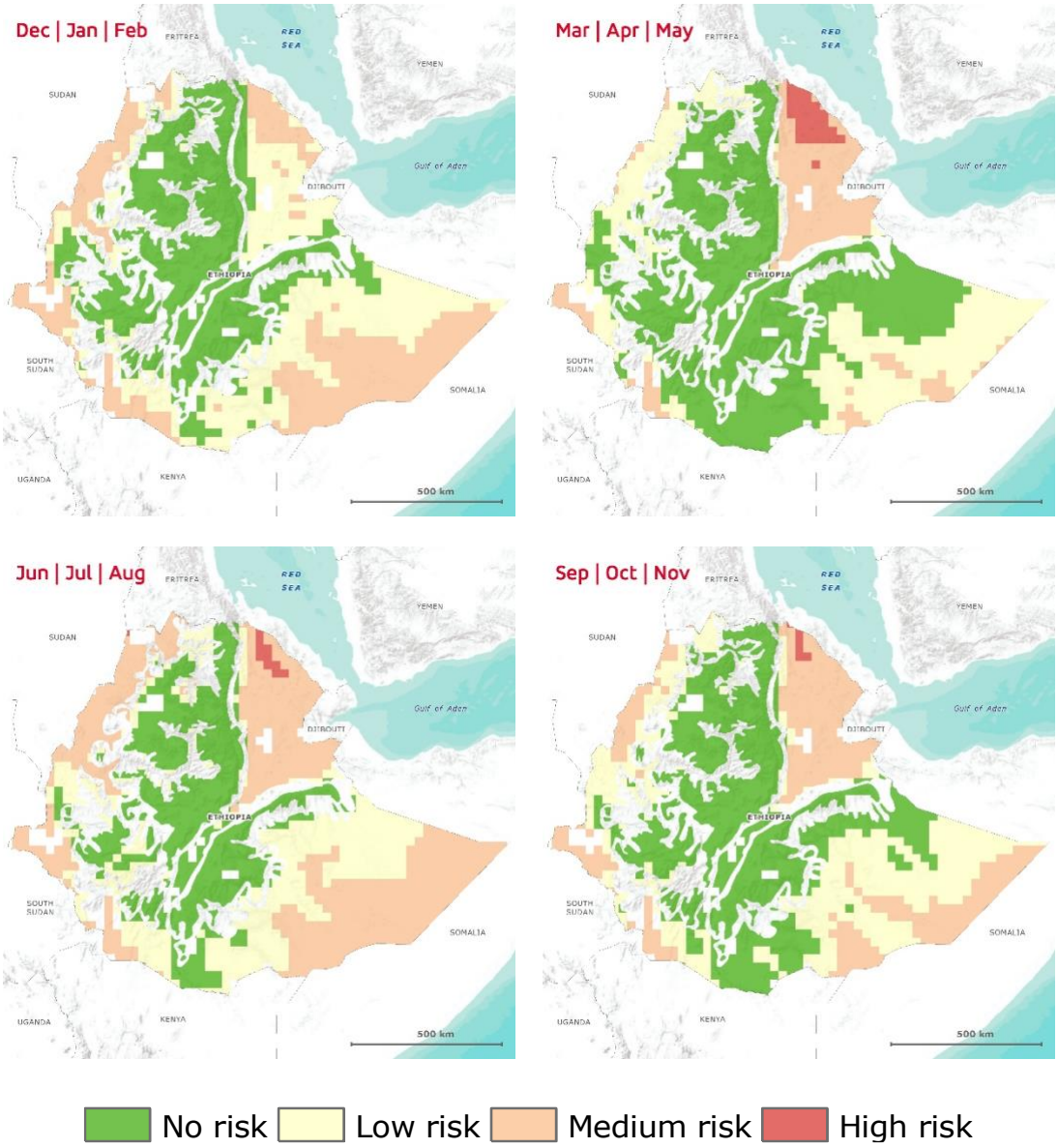

Figure 3-14 Heat stress index in Ethiopia per season.

Results from Figure 3-14 are consistent with the map shown in Figure 3-15, where both cattle and goats show for 2021 the highest frequency of occurrence of moderate heat stress over the same region in the Northeast region, i.e., the deserts and xeric shrublands type of rangeland.

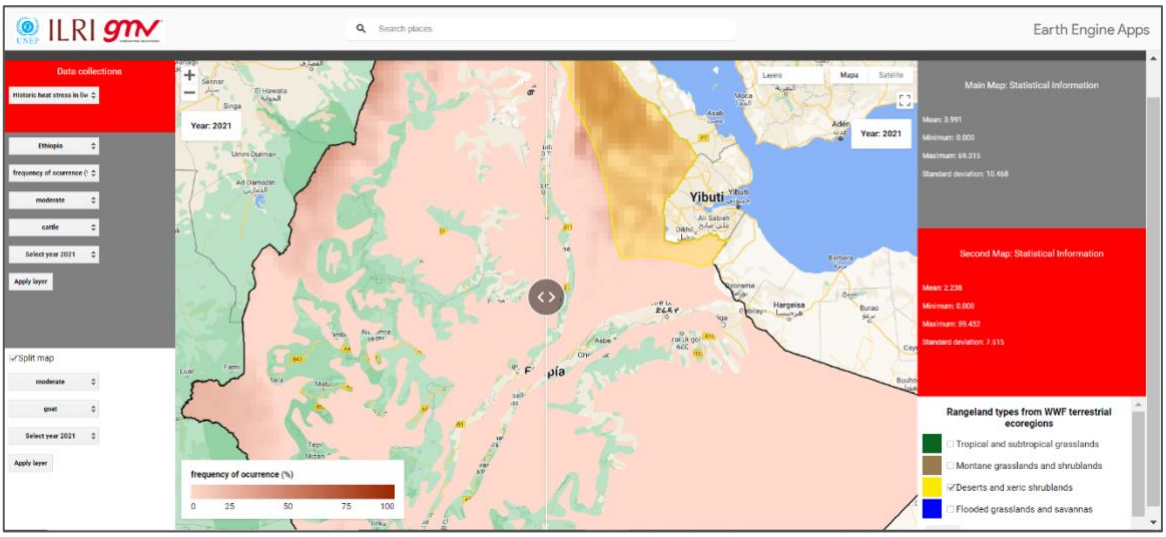

Figure 3-15 Snapshot of the moderate heat stress in cattle and goats for 2021 in Ethiopia with rangeland type deserts and xeric shrublands highlighted. Metrics correspond to the values for the entire country.

The heat stress risk index offers a nice opportunity to unbiasedly compare the livestock risk over the country or across countries. In Figure 3-16, the highest risk for livestock identified by 2021 in the country is in the northern region of Afar region. This is computed normalizing the heat stress results for different species by the global livestock density distribution by 2015 from FAO. The overall risk of Ethiopia can be compared with the results obtained for Senegal. As shown in Figure 3-17, most of the country is under medium risk while Ethiopia shows low risk for most of the regions. However, no regions under high risk have been observed in Senegal in contrast to the desert areas of Ethiopia.

The same comparison but using the CORDEX projections shows the results depicted in Figure 3-18 and Figure 3-19. Under the scenario given by the RCP 8.5 in the period 2070-2098 the heat stress risk seriously worsens for both countries, but the changes over Senegal are striking as the complete country transitions from medium to high risk.

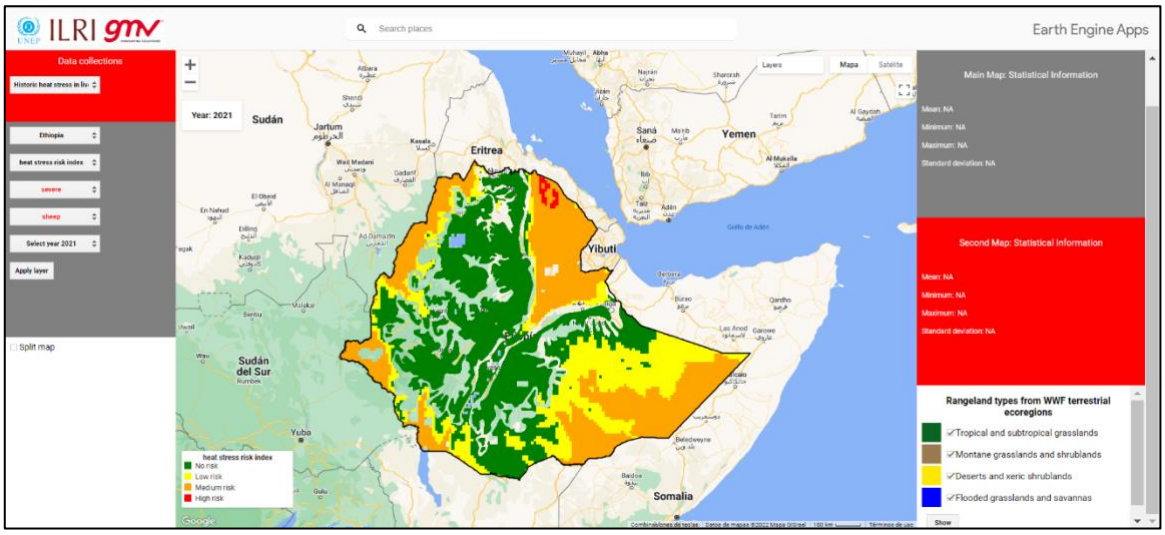

Figure 3-16 Snapshot of the heat stress risk index for Ethiopia by 2021.

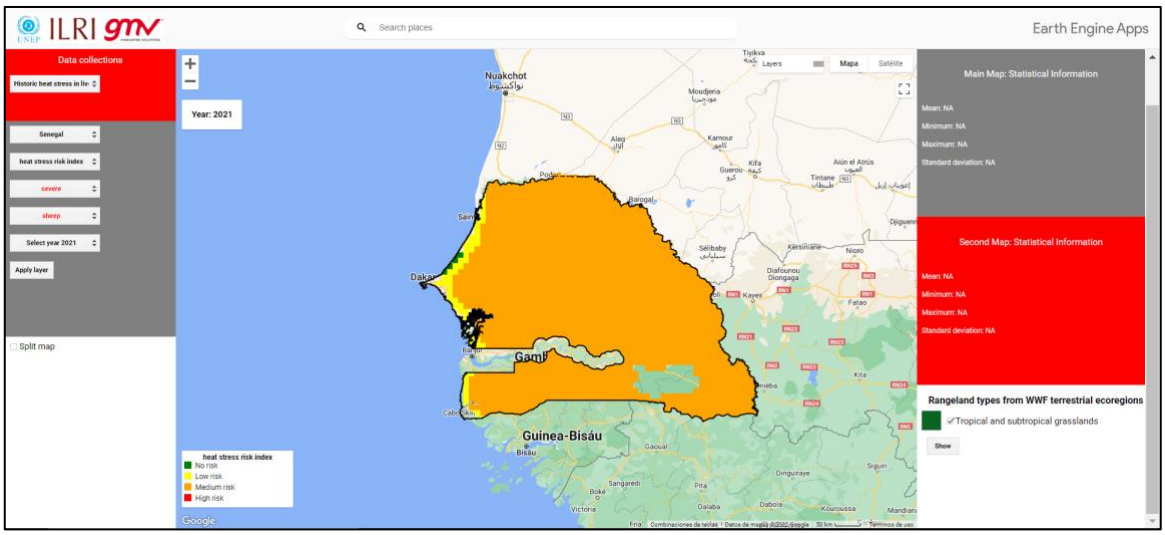

Figure 3-17 Snapshot of the heat stress risk index for Senegal by 2021.

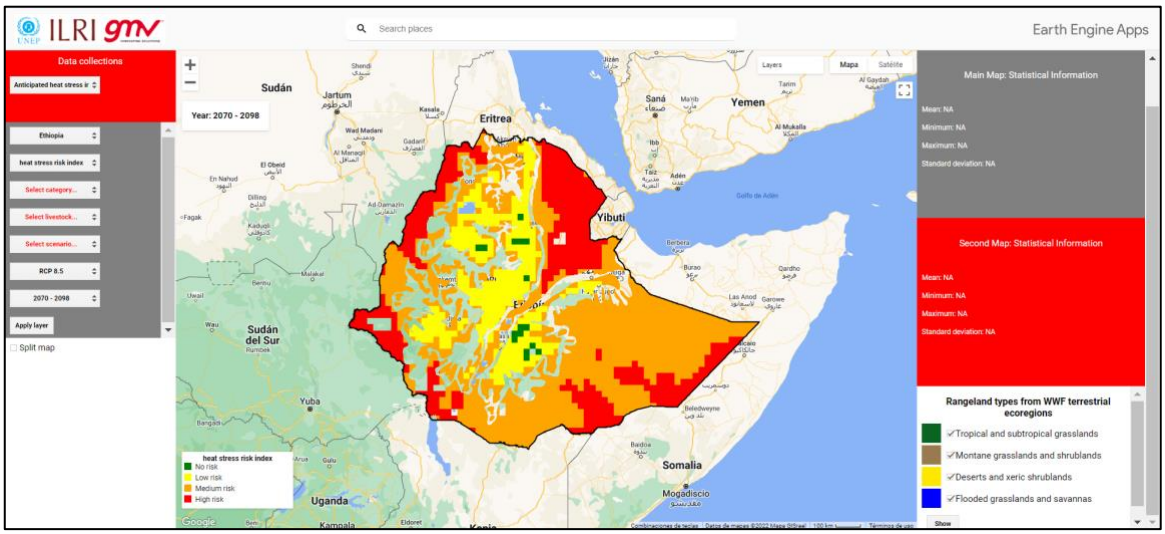

Figure 3-18 Snapshot of the heat stress risk index for Ethiopia by 2098 (RCP 8.5).

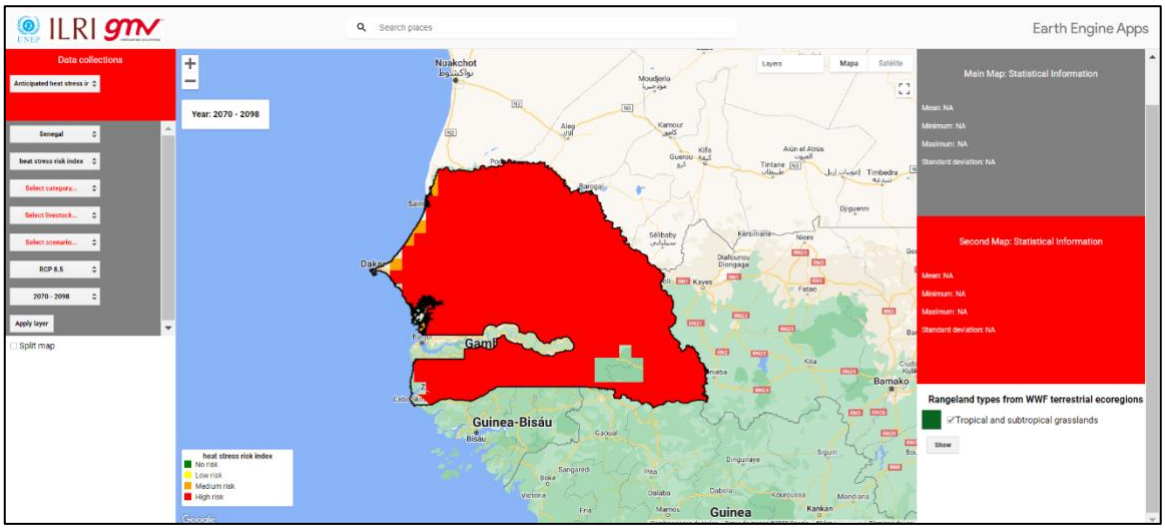

Figure 3-19 Snapshot of the heat stress risk index for Senegal by 2098 (RCP 8.5).

Figure 3-22 and Figure 3-23 shows the anticipated heat stress in cattle for the period 2070-2098 in consecutive days and frequency of occurrence, respectively.

The heat stress in livestock will be seriously aggravated due to climate change as it can be seen by comparing the results for 2021 shown in Figure 3-20. Under the scenario RCP 2.6 the increase is very significant, but the RCP 8.5 presents a scenario where all the cattle in the country is at least under moderate heat stress during the entire year.

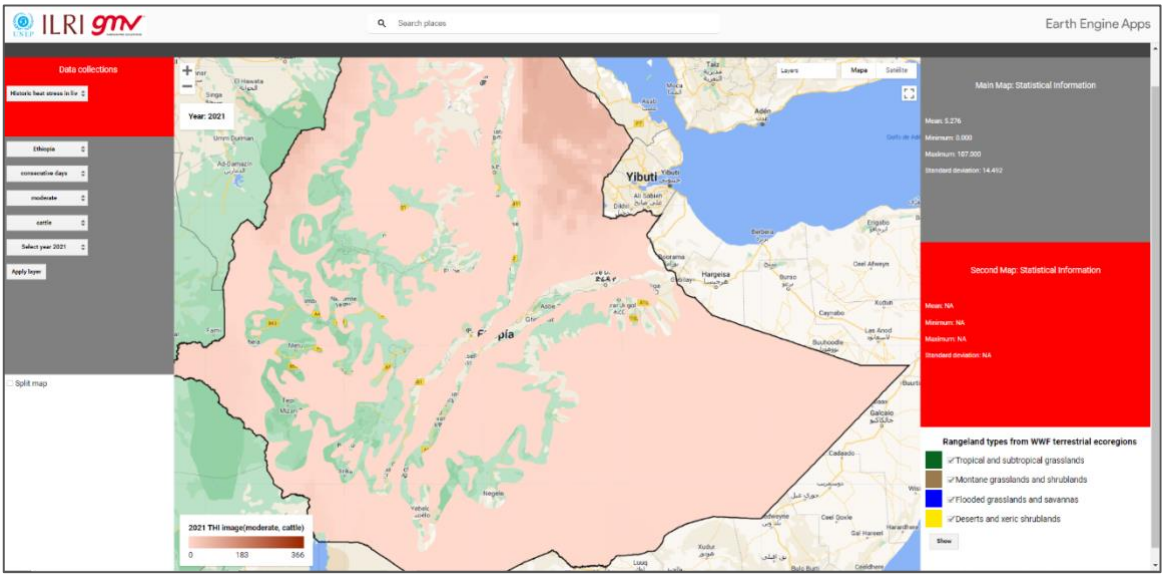

Figure 3-20 Snapshot of the moderate heat stress in cattle for 2021 in Ethiopia.

The human appropriation of net primary productivity (HANPP) provides a useful measure of human intervention into the productive ecosystems. The project team calculated the HANPP derived from grazing activities over Africa by using results from global dynamic vegetation models, Earth Observation satellites and country statistics from FAO. Note that grazing activities consider harvesting crops to feed livestock.

This dataset is highly experimental as uses a novel approach combining model and satellite data. The product is expected to be further developed and once validated, included into the web-based app platform.

Figure 3-21 shows the human appropriation of net primary productivity from livestock production over Ethiopia as a percentage of potential net primary production (NPP_0) derived from models. Blue (negative values) indicates increases of NPP_t (the fraction of NPP remaining in rangelands after grazing) over NPP_0, yellow indicates low HANPP, and red colours indicate medium to high HANPP.

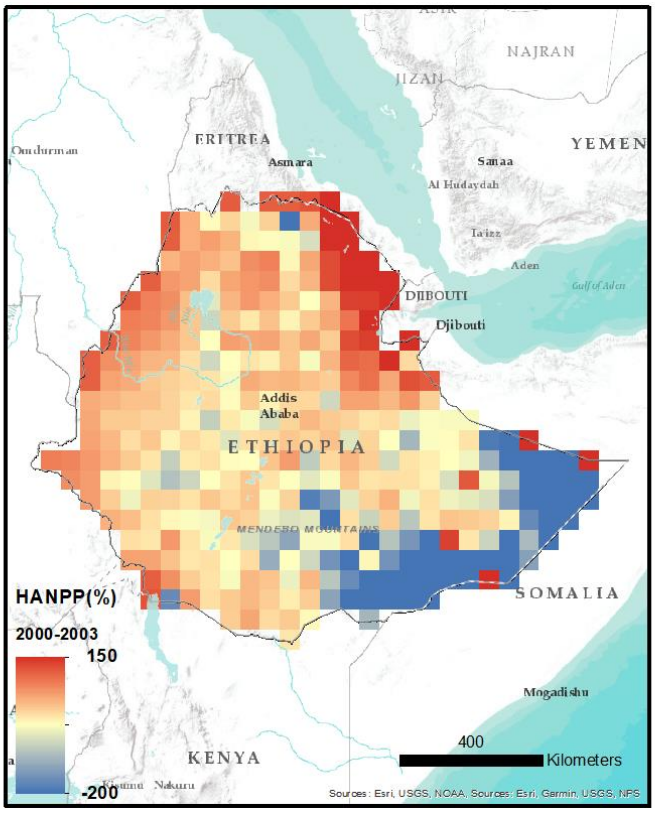

Figure 3-21 Human appropriation of net primary productivity including only human-induced livestock grazing over Ethiopia as a percentage of potential net primary production (NPP_0).

RCP 2.6

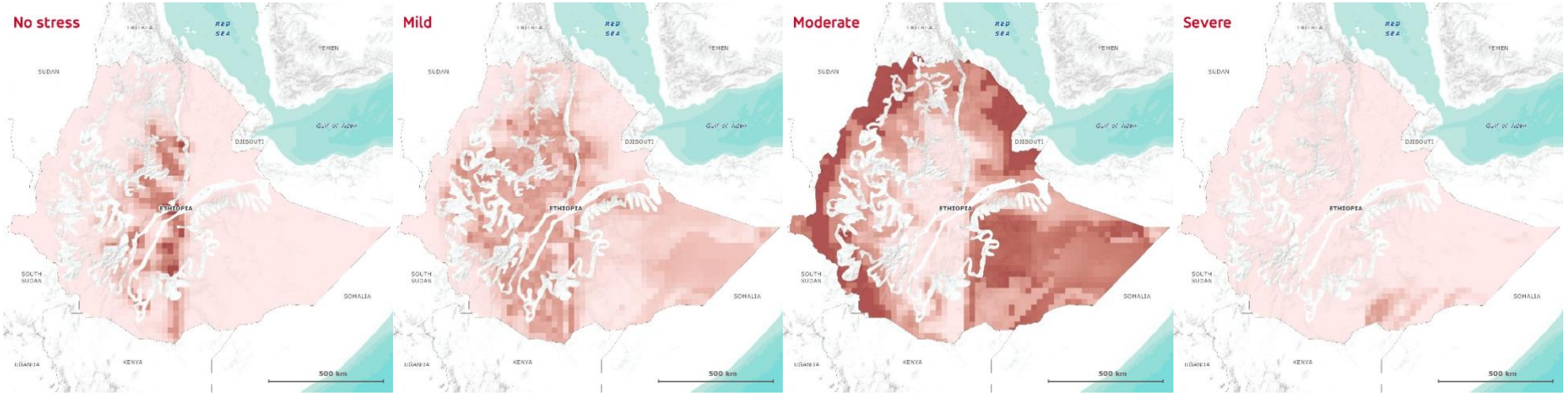

RCP 8.5

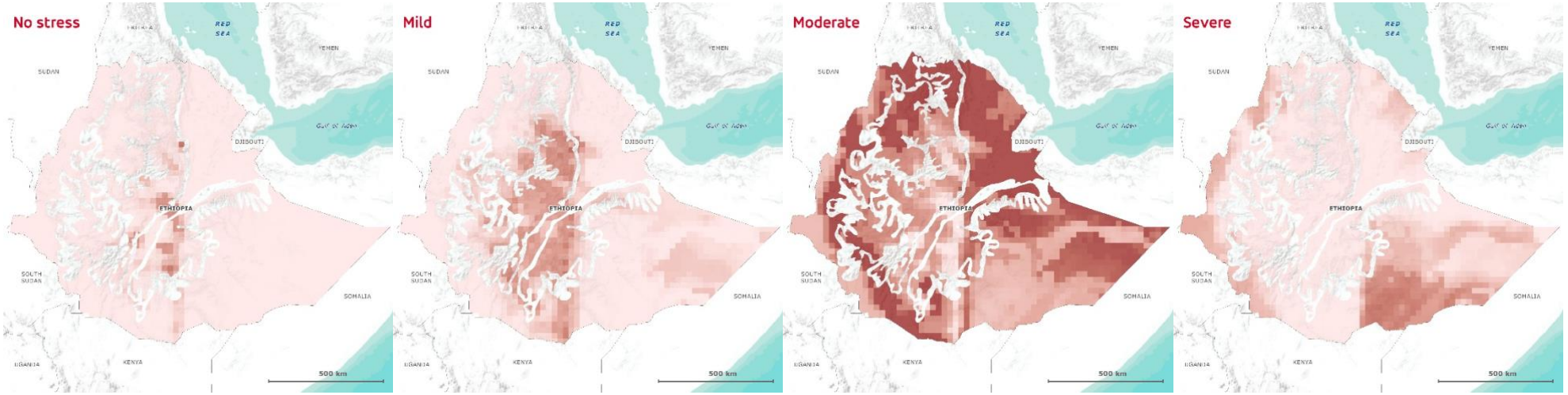

Figure 3-22 Expected heat stress in cattle for the period 2070-2090 for both RCP 2.6 and 8.5 expressed in consecutive days.

Anticipated heat stress in livestock / Consecutive days / Cattle

Period: 2070-2098

RCP 2.6

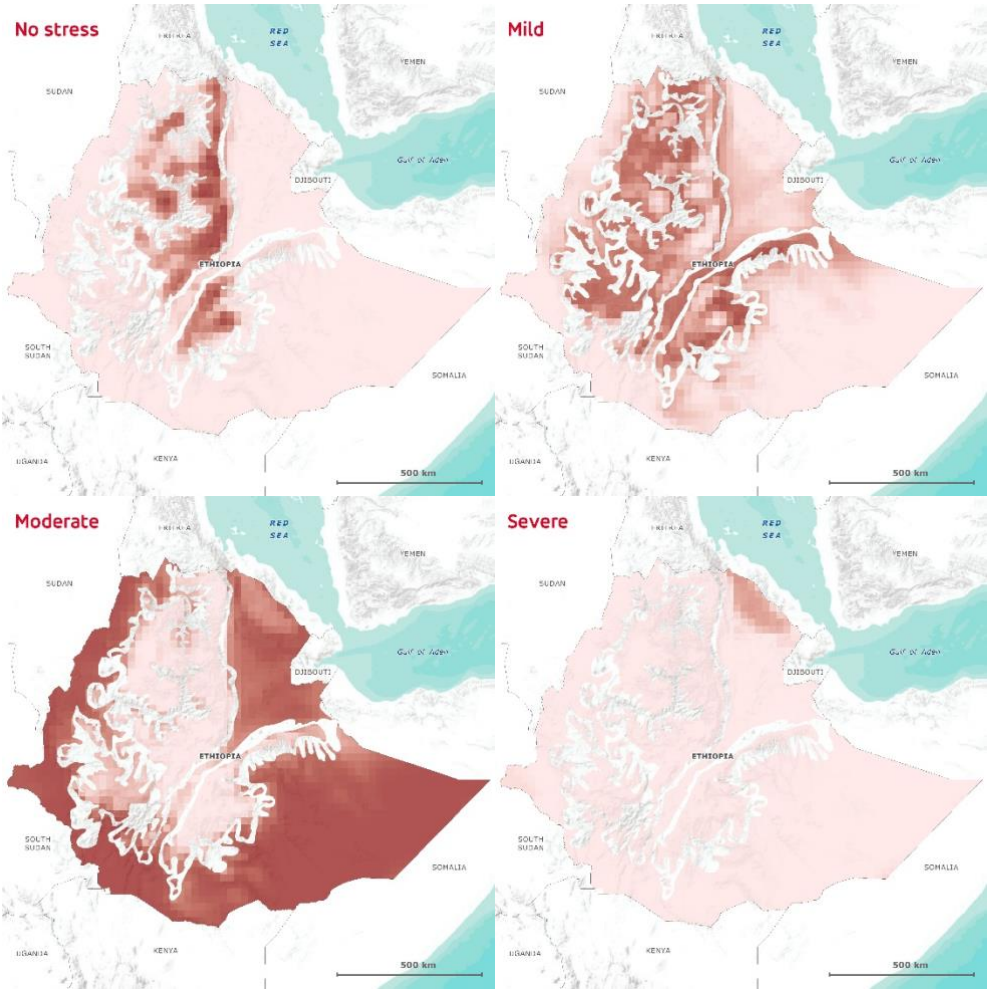
No stress
Mild
Moderate
Severe
RED SEA
YEMEN
SUDAN
DJIBOUTI
ETHIOPIA
SOUTH SUDAN
SOMALIA
KENYA
UGANDA
500 km

RCP 8.5

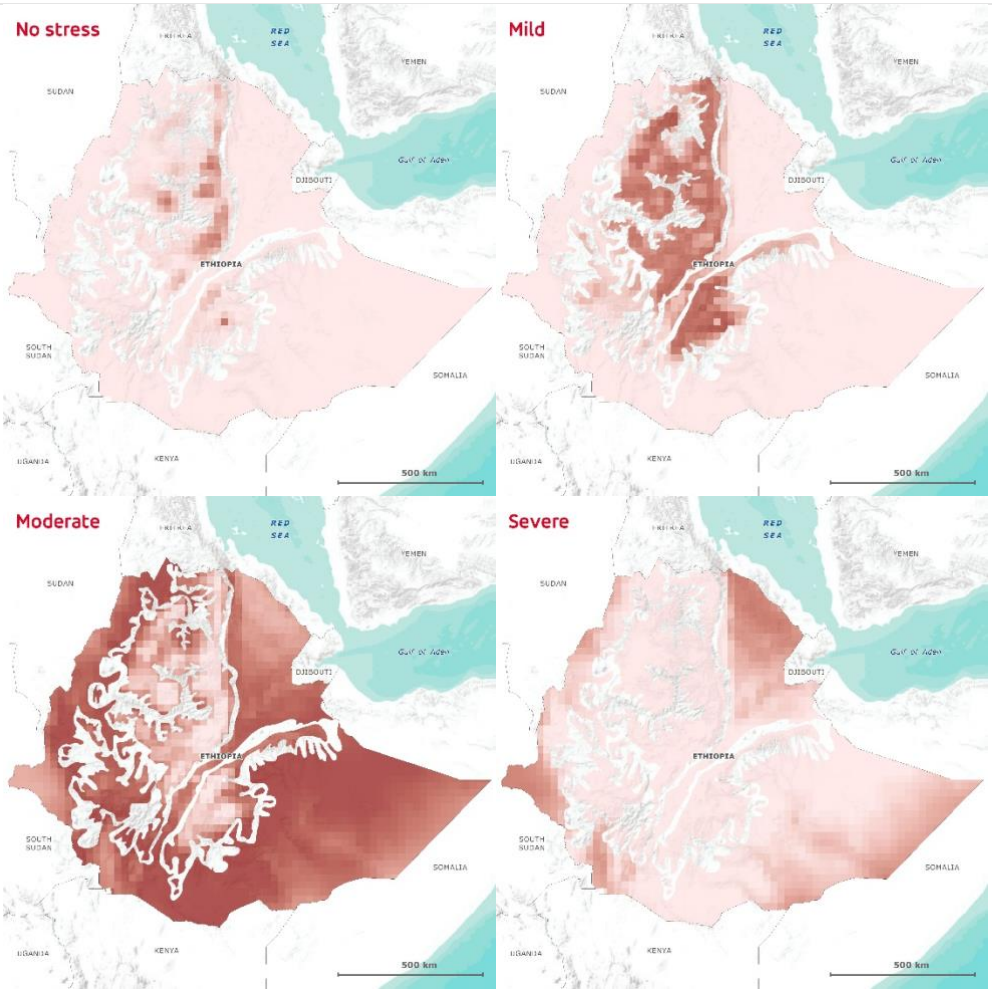

Figure 3-23 Expected heat stress in cattle for the period 2070-2090 for both RCP 2.6 and 8.5 expressed in frequency of occurrence.